

# On the cellular instability of flames near porous-plug burners

By A. C. MCINTOSH

College of Aeronautics,† Cranfield Institute of Technology, Cranfield, Bedford, U.K.

(Received 7 August 1984)

Two-dimensional burner-flame stability is discussed with arbitrary gas expansion. Density variations are allowed for by fully coupling the continuity and momentum equations. The flame is assumed to be close to a porous-plug-type flameholder so that the conventional hydrodynamic zone upstream of the flame cannot be included. Instead, the flow is assumed to obey a Darcy-type law within the holder, relating pressure gradient and velocity. It is shown that the influence of the holder and the acceleration due to gravity are important factors governing the onset of cellularity in porous-plug burner flames. Further, the balance of the transverse and longitudinal Darcy constants used to describe the upstream hydrodynamic zone within the holder have a vital effect on stability predictions. Experimental observations are confirmed by the theory presented.

---

## 1. Introduction

In much of the recent work on flame stability, a fundamental building block is the method of matched asymptotic expansions based on large activation energy. Such methods rely in general on the concept of an overall reaction governing flame behaviour. A striking confirmation of the usefulness of the overall reaction scheme has been given in a recent paper by Coffee, Kotlar & Miller (1983). The predictions of species concentration, temperature, flame speed and heat release of three types of steady planar premixed flames (ozone/oxygen, hydrogen/air and methane/air) are carefully compared using first a detailed chemistry model, and then a one-reaction model. The agreements between the two approaches are marked, and this excellent work has given renewed confidence to the relevance of theories of unsteady flames based on global reaction schemes.

Since the important work of Pelcé & Clavin (1982), considerable progress has been made in modelling curved flames in uniform and non-uniform flows. The basis of such theories is that the transverse wavelength of the curved flame is large compared with a typical diffusion length. Fluctuations in pressure, velocity, temperature and species have then been considered in large hydrodynamic zones before and after the flame, and it is now possible to consider the fluid-dynamic interaction of flames with quite complicated flows (Matalon & Matkowsky 1982).

In considering the stability of plane flames to planar and transverse disturbances, theories including the effect of hydrodynamics have considered the flame to be 'free' and away from solid boundaries. The advantage of the burner-flame model discussed in detail in Clarke & McIntosh (1980) is twofold. First, it enables localized and

† Present address: Department of Mathematics and Computation, Luton College of Higher Education, Park Square, Luton, Bedfordshire, U.K.

experimentally realizable heat losses to be modelled without the need to alter the Arrhenius term and thereby sidestep the cold-boundary difficulty. Secondly, it enables the 'free' flame to be approached in a rational manner as a special case of the physically appealing burner-flame model. This matter is discussed in some depth in the recent review article by Kassoy (1985), who shows that the classical concept of a freely propagating flame should really only be viewed in this context.

In this paper we proceed to investigate the two-dimensional stability of burner flames without any gross assumptions concerning the velocity field. Since at all times the flame is not considered to be more than a few diffusion lengths away from the burner surface, an upstream hydrodynamic zone is not included in the analysis. Instead, conditions at the burner surface are established by considering the flow within the porous plug to follow a Darcy-type law where the velocity is assumed to be proportional to the pressure gradient. The conductance of the flameholder is considered large, so that temperature (and hence density) fluctuations are negligible. The pressure and two components of velocity within the holder then obey Laplace's equation. Thus the mathematical model allows for an upstream hydrodynamic zone *within* the holder which, along with the influence of gravitational acceleration, has a considerable effect on the onset of flame cellularity.

The work presented here is based on the one-dimensional theory of McIntosh & Clarke (1984*b*, referred to hereinafter as I), but extended to two dimensions. Recently, Buckmaster (1983) has published a stability theory for burner flames which assumes the flame is immersed in a constant velocity field. This comes about by assuming that density variations are negligible. Such an assumption has produced some useful simplifications in previous work, and led to important advances in the understanding of diffusional thermal instabilities. However, when fluid-dynamical effects become important (as here within the flameholder), then such an assumption cannot be made. In reality, the density variations can be considerable, and thus here the assumption is employed that density is inversely proportional to temperature. One other important difference is that we make no *a priori* restriction on Lewis number. As explained in detail in I, this parameter can be considered simply  $O(1)$  throughout, and need not be expanded in terms of inverse activation energy  $\theta_1^{-1}$ .

In keeping with I, we adopt a very definite order in taking limits. There are three parameters involved: (i)  $\epsilon$ , the measure of perturbations of the flame; (ii)  $\theta_1$ , the activation energy; and (iii)  $k$ , the wavenumber (proportional to diffusion length over wavelength and a measure of the two-dimensionality of the flow). In this work the  $\epsilon \rightarrow 0$  limit is taken first (§2), with the assumption  $\theta_1 \epsilon \rightarrow 0$  in that limit. This assumption is necessary since the product  $\theta_1 \epsilon$  is explicitly encountered when the reaction term is perturbed. The  $\theta_1^{-1} \rightarrow 0$  limit is then taken (§3), which effectively replaces the Arrhenius chemical source term with jump conditions across the flame in terms of  $\theta_1$ . At this stage in the argument the problem reduces to the solution of a set of ordinary second-order differential equations with non-constant coefficients (owing to the assumption of non-zero gas expansion). Such a problem could be analysed numerically, but to give some idea of the solution we have made the preheat equations tractable by treating  $k$  as small and developing series solutions up to order  $k^2$ , in much the same way as Pelcé & Clavin (1982) (see §4). A dispersion relation between complex frequency  $\omega$  and wavenumber  $k$  is then obtained and used to determine, in particular, the onset of cellular instability for different values of the eight parameters,  $Le$  (Lewis number),  $Pr$  (Prandtl number),  $\theta_1 B_1^*$  (reduced activation energy),  $x_{1f_1}$  (mass-weighted stand-off distance),  $T_{01}$  (a measure of the gas expansion ratio),  $g_r$  (non-dimensionalized gravitational acceleration)  $\Omega_1$  and  $\Omega_2$  (flameholder

constants related to the fluid-dynamical effects of porosity). Section 5 discusses these results in the context of a typical propane/air flame burning near a porous flameholder. The results are displayed in figure 7, where the onset of cellularity is shown to agree well with that obtained in the experiments of Botha & Spalding (1954).

## 2. Formulation

### 2.1. Assumptions and basic equations

The combustion is assumed to take place in a gas stream of low velocity near a flameholder. (Figure 1 shows a schematic of the initially steady flame.) Near-isobaric conditions are thus assumed, with pressure variations  $O(M^2)$ , where  $M$  is the Mach number of the flow. Thus

$$p = 1 + M^2 p_r. \quad (1)$$

In this equation, as in all subsequent analysis, all variables, except temperature, are non-dimensionalized with respect to steady upstream conditions. Temperature is non-dimensionalized with respect to its steady value in the burnt stream.

In formulating the governing equations for a premixed flame under unsteady conditions in two dimensions, we specifically avoid the constant-density approximation, and replace it with the more realistic assumption that

$$\rho\lambda = 1, \quad (2)$$

where  $\rho$  and  $\lambda$  are the non-dimensional density and thermal conductivity respectively. For near-isobaric conditions, this effectively implies that thermal conductivity is proportional to temperature  $T$ . In practice,  $\lambda \propto T^h$ :  $0.75 \leq h \leq 0.94$  (see Hirschfelder, Curtiss & Bird 1954; Kanury 1975), so that equation (2) is a good approximation.

Assuming that the diffusion process can be described by a single limiting-species mass diffusion coefficient and that a simple Fick law of diffusion is obeyed, there is a constant Lewis number throughout the mixture which, following the definition of Markstein (1964; p. 26), is given by

$$Le \equiv \frac{\rho' D' C'_p}{\lambda'} = \frac{\rho'_{01} D'_{01} C'_p}{\lambda'_{01}}, \quad (3a)$$

where ' refers to dimensional quantities and the subscript '01' refers to the unburnt stream, and the specific heat of the mixture  $C'_p$  is assumed constant everywhere. The Prandtl number of the mixture is also assumed constant, so that

$$Pr \equiv \frac{\mu' C'_p}{\lambda'} = \frac{\mu'_{01} C'_p}{\lambda'_{01}}, \quad (3b)$$

where  $\mu'$  is the coefficient of dynamic viscosity. With the assumption of constant specific heat, the immediate implication from (3a, b) is that, in non-dimensional terms,

$$\rho D = \lambda, \quad \mu = \lambda. \quad (4a, b)$$

Using these relations, one can write down the equations of state, continuity, species, energy and momentum (in both longitudinal ( $x$ ) and transverse ( $y$ ) directions) as

$$\rho T = T_{01}, \quad (5)$$

$$\frac{\partial \rho}{\partial t} + \frac{\partial}{\partial x} (\rho u) + \frac{\partial}{\partial y} (\rho v) = 0, \quad (6)$$

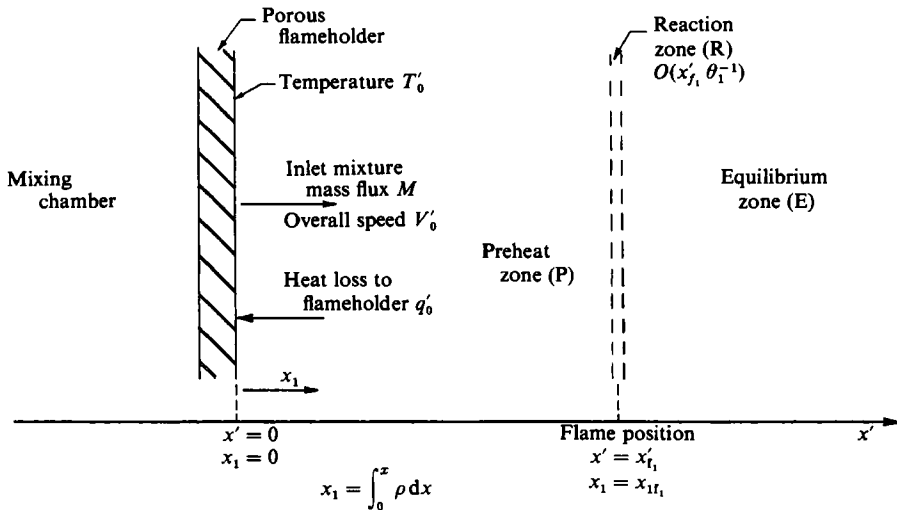


FIGURE 1. Schematic of initially plane flame with porous-plug flameholder.

$$\frac{\partial T}{\partial t} + u \frac{\partial T}{\partial x} + v \frac{\partial T}{\partial y} - \frac{1}{Le \rho} \frac{\partial}{\partial x} \left( \lambda \frac{\partial T}{\partial x} \right) - \frac{1}{Le \rho} \frac{\partial}{\partial y} \left( \lambda \frac{\partial T}{\partial y} \right) = \frac{Le(1+\sigma)Q_1}{\sigma} A_1 C_\ell C_r \exp \left[ \theta_1 \left( 1 - \frac{1}{T} \right) \right], \quad (7)$$

$$\frac{\partial C_\ell}{\partial t} + u \frac{\partial C_\ell}{\partial x} + v \frac{\partial C_\ell}{\partial y} - \frac{1}{\rho} \frac{\partial}{\partial x} \left( \lambda \frac{\partial C_\ell}{\partial x} \right) - \frac{1}{\rho} \frac{\partial}{\partial y} \left( \lambda \frac{\partial C_\ell}{\partial y} \right) = -Le A_1 C_\ell C_r \exp \left[ \theta_1 \left( 1 - \frac{1}{T} \right) \right], \quad (8)$$

$$\frac{\partial u}{\partial t} + u \frac{\partial u}{\partial x} + v \frac{\partial u}{\partial y} + \frac{1}{\gamma \rho} \frac{\partial p_r}{\partial x} = -g_r + \frac{Sc}{\rho} \left[ \frac{\partial}{\partial x} \left( \lambda \frac{\partial u}{\partial x} \right) + \frac{\partial}{\partial y} \left( \lambda \frac{\partial u}{\partial y} \right) + \frac{1}{3} \frac{\partial}{\partial x} \left( \lambda \frac{\partial u}{\partial x} + \lambda \frac{\partial v}{\partial y} \right) + \frac{\partial}{\partial y} \left( \lambda \frac{\partial v}{\partial x} \right) - \frac{\partial}{\partial x} \left( \lambda \frac{\partial v}{\partial y} \right) \right], \quad (9a)$$

$$\frac{\partial v}{\partial t} + u \frac{\partial v}{\partial x} + v \frac{\partial v}{\partial y} + \frac{1}{\gamma \rho} \frac{\partial p_r}{\partial y} = \frac{Sc}{\rho} \left[ \frac{\partial}{\partial x} \left( \lambda \frac{\partial v}{\partial x} \right) + \frac{\partial}{\partial y} \left( \lambda \frac{\partial v}{\partial y} \right) + \frac{1}{3} \frac{\partial}{\partial y} \left( \lambda \frac{\partial u}{\partial x} + \lambda \frac{\partial v}{\partial y} \right) + \frac{\partial}{\partial x} \left( \lambda \frac{\partial u}{\partial y} \right) - \frac{\partial}{\partial y} \left( \lambda \frac{\partial u}{\partial x} \right) \right]. \quad (9b)$$

In these equations  $u$  and  $v$  are respectively the longitudinal and transverse components of velocity,  $C_\ell$ ,  $C_r$  refer to lean and rich species mass fractions,  $\theta_1$  is activation energy (referred to initial burnt temperature),  $\sigma$  the ratio of molecular weights,  $Q_1$  the reduced heat of reaction,  $Sc$  the flow Schmidt number ( $= Pr/Le$ ),  $\gamma$  the ratio of specific heats and  $A_1$  the steady, pre-exponential eigenvalue. This quantity is typically (for far-from-stoichiometric conditions – see Clarke & McIntosh 1980) proportional to  $\theta_1^2$ . In the non-dimensionalizing of (5)–(9) characteristic values of diffusion length and time have been used and, in particular, the gravitational acceleration term  $g_r$  in the longitudinal momentum balance is related to the dimensional acceleration  $g'$  by

$$g_r \equiv g' D'_{01} / u'_{01}{}^3. \quad (10)$$

The equations and boundary conditions are an extension to two dimensions of the work described in I. Thus the upstream condition on species is the Hirschfelder condition

$$C_\ell(0, y, t) - \frac{1}{M_0} \left( \frac{\partial C_\ell}{\partial x} \right)_{0, y, t} = \text{const}, \quad (11)$$

and the conductance of the holder is assumed large, so that temperature fluctuations are absorbed. Hence

$$T_0 \equiv T(0, y, t) = \text{const} = T_{01}, \quad (12)$$

and with isobaric conditions it follows that density is also constant. Thus

$$\rho_0 \equiv \rho(0, y, t) = \text{const} = 1. \quad (13)$$

Note that in (11)  $M_0$  is the longitudinal mass flux downstream of the holder, so that

$$M_0 \equiv \rho_0 u_0 = u_0. \quad (14)$$

The conditions on pressure and velocity at the holder surface derive from considering the flow through the porous material of the holder. This is discussed in detail in Appendix A. It is shown that for small harmonic perturbations in  $O(M^2)$  pressure ( $p_u \exp(\omega t + iky)$ ), longitudinal velocity ( $U_u \exp(\omega t + iky)$ ) and transverse velocity ( $V_u \exp(\omega t + iky)$ ) at the downstream face of the holder,  $U_u(0)$  and  $V_u(0)$  are related to  $p_u(0)$  by the equations

$$U_u(0) = -\Omega_3 k \frac{p_u(0)}{\gamma} = M_u(0), \quad (15a, b)$$

$$V_u(0) = -\Omega_2 k \frac{p_u(0)}{\gamma}, \quad (16)$$

where

$$\Omega_3 \equiv \beta(\Omega_1 \Omega_2)^{\frac{1}{2}}, \quad (17)$$

and  $\Omega_1, \Omega_2$  are the non-dimensionalized Darcy constants in the longitudinal and transverse directions respectively.  $\beta$  is the porosity of the holder. In practice  $\beta$  and the ratio  $\Omega_2/\Omega_1$  will be specified.  $\Omega_1$  will also be known and is directly proportional to the square of the pore diameter. In Appendix A it is shown that a good approximation is

$$\Omega_1 = \frac{8d'^2 u_{01}'^2}{Le Pr K_{01}'^2}, \quad (18)$$

where  $d'$  is a measure of the pore size, and  $K_{01}'$  is the thermal diffusivity ( $= \lambda_{01}'/\rho_{01}' C_p'$ ).

Downstream, the conditions are simply that all variables take on their initial (steady) values.

It should be pointed out here that it is the boundary conditions at the upstream end of the preheat zone that cause this work to diverge from the model proposed by Pelcé & Clavin (1982). In that paper they were dealing with essentially 'free' flames, and allowed for variations in all quantities far upstream on a hydrodynamic lengthscale. In our case we are dealing with a somewhat different problem where any fluctuations upstream are transmitted to a hydrodynamic zone *within* the holder itself. As pointed out by McIntosh & Clarke (1984a) and Buckmaster (1983), the thermal inertia of a real burner is large and will absorb any temperature fluctuations. However, velocity and pressure fluctuations do not follow the same pattern, and continue into the holder. Because this upstream hydrodynamic zone is not the same type

as that found ahead of 'free' flames (such as in Pelcé & Clavin 1982), the twin-scaling approach advocated in that paper is not adopted here.

Since we are shortly to consider only small perturbations in the  $Y$ -direction, it is convenient to transform the  $x$ -coordinate to the mass-weighted variable

$$x_1 = \int_0^x \rho \, dx, \quad (19)$$

and, noting that  $C_r$  is related to  $C_\ell$  through the mixture strength constant  $|A_1|$ , i.e.

$$C_r = C_\ell + |A_1|, \quad (20)$$

(5)–(9) transform to

$$\rho T = T_{01}, \quad (21)$$

$$(M_0 - W) \frac{\partial \rho}{\partial x_1} + \frac{\partial \rho}{\partial t} + \rho^2 \frac{\partial u}{\partial x_1} + H \frac{\partial}{\partial x_1} (\rho v) + \frac{\partial}{\partial y} (\rho v) = 0, \quad (22)$$

$$(M_0 - W) \frac{\partial T}{\partial x_1} + \frac{\partial T}{\partial t} + v \frac{\partial T}{\partial y} + v H \frac{\partial T}{\partial x_1} - \frac{1}{Le} \frac{\partial^2 T}{\partial x_1^2} - \frac{1}{Le \rho} \left( H \frac{\partial}{\partial x_1} + \frac{\partial}{\partial y} \right) \lambda \left( H \frac{\partial T}{\partial x_1} + \frac{\partial T}{\partial y} \right) \\ = \frac{Le(1+\sigma)Q_1}{\sigma} A_1 C_\ell (C_\ell + |A_1|) \exp \left[ \theta_1 \left( 1 - \frac{1}{T} \right) \right], \quad (23)$$

$$(M_0 - W) \frac{\partial C_\ell}{\partial x_1} + \frac{\partial C_\ell}{\partial t} + v \frac{\partial C_\ell}{\partial y} + v H \frac{\partial C_\ell}{\partial x_1} - \frac{\partial^2 C_\ell}{\partial x_1^2} - \frac{1}{\rho} \left( H \frac{\partial}{\partial x_1} + \frac{\partial}{\partial y} \right) \lambda \left( H \frac{\partial C_\ell}{\partial x_1} + \frac{\partial C_\ell}{\partial y} \right) \\ = -Le A_1 C_\ell (C_\ell + |A_1|) \exp \left[ \theta_1 \left( 1 - \frac{1}{T} \right) \right], \quad (24)$$

$$(M_0 - W) \frac{\partial u}{\partial x_1} + \frac{\partial u}{\partial t} + v H \frac{\partial u}{\partial x_1} + v \frac{\partial u}{\partial y} + \frac{1}{\gamma} \frac{\partial p_\ell}{\partial x_1} \\ = -g_r + Sc \frac{\partial^2 u}{\partial x_1^2} + \frac{Sc}{\rho} \left( H \frac{\partial}{\partial x_1} + \frac{\partial}{\partial y} \right) \lambda \left( H \frac{\partial u}{\partial x_1} + \frac{\partial u}{\partial y} \right) + \frac{1}{3} Sc \frac{\partial^2 u}{\partial x_1^2} \\ - \frac{2}{3} Sc \frac{\partial}{\partial x_1} \left( \lambda \left( H \frac{\partial v}{\partial x_1} + \lambda \frac{\partial v}{\partial y} \right) \right) + \frac{Sc}{\rho} H \frac{\partial^2 v}{\partial x_1^2} + \frac{Sc}{\rho} \frac{\partial^2 v}{\partial x_1 \partial y}, \quad (25)$$

$$(M_0 - W) \frac{\partial v}{\partial x_1} + \frac{\partial v}{\partial t} + v H \frac{\partial v}{\partial x_1} + v \frac{\partial v}{\partial y} + \frac{1}{\gamma \rho} \left( H \frac{\partial}{\partial x_1} + \frac{\partial}{\partial y} \right) p_\ell \\ = Sc \frac{\partial^2 v}{\partial x_1^2} + \frac{Sc}{\rho} \left( H \frac{\partial}{\partial x_1} + \frac{\partial}{\partial y} \right) \lambda \left( H \frac{\partial v}{\partial x_1} + \frac{\partial v}{\partial y} \right) \\ + \frac{Sc}{3\rho} \left( H \frac{\partial}{\partial x_1} + \frac{\partial}{\partial y} \right) \left( \frac{\partial u}{\partial x_1} + \lambda H \frac{\partial v}{\partial x_1} + \lambda \frac{\partial v}{\partial y} \right) \\ + Sc \frac{\partial}{\partial x_1} \left( \lambda \left( H \frac{\partial u}{\partial x_1} + \frac{\partial u}{\partial y} \right) \right) - \frac{Sc}{\rho} H \frac{\partial^2 u}{\partial x_1^2} - \frac{Sc}{\rho} \frac{\partial^2 u}{\partial x_1 \partial y}, \quad (26)$$

where  $H$  and  $W$  are defined by

$$H \equiv \int_0^x \frac{\partial \rho}{\partial y} \, dx, \quad (27)$$

$$W \equiv \int_0^{x_1} \frac{\partial}{\partial y} (\rho v) \, dx. \quad (28)$$

## 2.2. Small perturbations

We now consider each of the seven variables  $T, C_\ell, \rho, u, v, p_\ell, \lambda$  to be perturbed from its initial steady value. The small (order- $\epsilon$ ) perturbations are restricted to be such that

$$\epsilon \ll \theta_1^{-1}, \quad (29)$$

and thus we follow closely the analysis of the earlier paper (I), where a perturbation analysis of the one-dimensional equations was made. The perturbations here are in all seven variables, with

$$X(x_1, y, t) = X_s(x_1) + \epsilon X_u(x_1) \exp(\omega t + ik y) \quad (X = T, C_\ell, \rho, u, v, p_\ell, \lambda), \quad (30)$$

and  $\omega$  and  $k$  are respectively complex frequency and wavenumber for (unforced) harmonic disturbances in two dimensions.

Equations (2) and (4) immediately imply that, to leading order in  $\epsilon$ ,

$$\rho_u = -\frac{T_{01}}{T_s^2} T_u, \quad \lambda_u = \frac{T_u}{T_{01}}, \quad (31), (32)$$

and it can be shown (after a considerable amount of algebraic manipulation) that (22)–(26) yield the following linearized perturbation equations in the remaining five variables  $T_u, C_{\ell u}, U_u, V_u, p_u$ :

$$\omega T_u + \frac{dT_u}{dx_1} - (W_u - M_u(0)) \frac{dT_s}{dx_1} - T_{01} \frac{dU_u}{dx_1} - ik V_u T_s = 0, \quad (33)$$

$$\begin{aligned} \omega T_u + \frac{dT_u}{dx_1} - \frac{1}{Le} \frac{d^2 T_u}{dx_1^2} - (W_u - M_u(0)) \frac{dT_s}{dx_1} - \frac{1}{Le} \frac{T_s^2}{T_{01}^2} \left( ik \frac{dT_s}{dx_1} H_u - k^2 T_u \right) \\ = \frac{Le(1+\sigma) Q_1}{\sigma} R_u, \end{aligned} \quad (34)$$

$$\omega C_{\ell u} + \frac{dC_{\ell u}}{dx_1} - \frac{d^2 C_{\ell u}}{dx_1^2} - (W_u - M_u(0)) \frac{dC_{\ell s}}{dx_1} - \frac{T_s^2}{T_{01}^2} \left( ik \frac{dC_{\ell s}}{dx_1} H_u - k^2 C_{\ell u} \right) = -Le R_u, \quad (35)$$

$$\begin{aligned} \omega U_u + \frac{dU_u}{dx_1} + \frac{1}{\gamma} \frac{dp_u}{dx_1} - \frac{1}{T_{01}} (W_u - M_u(0)) \frac{dT_s}{dx_1} \\ = \frac{4}{3} Sc \frac{d^2 U_u}{dx_1^2} - \frac{2}{3} \frac{Sc}{T_{01}} ik \frac{d}{dx_1} (T_s V_u) + \frac{ik Sc T_s}{T_{01}} \frac{dV_u}{dx_1} + \frac{Sc T_s^2}{T_{01}^2} \left( \frac{ik}{T_{01}} \frac{dT_s}{dx_1} H_u - k^2 U_u \right), \end{aligned} \quad (36)$$

$$\begin{aligned} \omega V_u + \frac{dV_u}{dx_1} + \frac{ik T_s}{\gamma T_{01}} p_u + \frac{Sc T_s}{T_{01}^2} H_u \frac{d^2 T_s}{dx_1^2} - \frac{T_s H_u}{T_{01}^2} \frac{dT_s}{dx_1} - \frac{T_s H_u}{T_{01}} g_r \\ = Sc \frac{d^2 V_u}{dx_1^2} - \frac{4}{3} \frac{k^2 Sc T_s^2}{T_{01}^2} V_u + \frac{ik Sc}{T_{01}} \frac{dT_s}{dx_1} U_u + \frac{Sc}{T_{01}^2} \frac{dT_s}{dx_1} \frac{d}{dx_1} (T_s H_u) + \frac{1}{3} \frac{ik Sc T_s}{T_{01}} \frac{dU_u}{dx_1}, \end{aligned} \quad (37)$$

where

$$H_u T_s = -ik \int_0^{x_1} T_u dx_1, \quad (38)$$

$$W_u = ik \int_0^{x_1} V_u dx_1, \quad (39)$$

$$R_u \equiv A_1 \left[ \frac{\theta_1 T_u}{T_s^2} (|A_1| + C_{\ell s}) C_{\ell s} + (|A_1| + 2C_{\ell s}) C_{\ell u} \right] \exp \left[ \theta_1 \left( 1 - \frac{1}{T_s} \right) \right]. \quad (40)$$

The boundary conditions upstream are

$$T_u(0) = 0, \quad (41)$$

$$C_{\ell u}(0) - \frac{dC_{\ell u}}{dx_1} \Big|_0 = -k\Omega_3 \frac{p_u(0)}{\gamma} B_1 \exp(-x_{1f_1}), \quad (42)$$

$$U_u(0) = -k\Omega_3 \frac{p_u(0)}{\gamma} = M_u(0), \quad (43)$$

$$V_u(0) = -ik\Omega_2 \frac{p_u(0)}{\gamma}, \quad (44)$$

where  $B_1$  is the heat-release parameter given by

$$B_1 \equiv \frac{1 - T_{01}}{1 - \exp(-Le x_{1f_1})} = \frac{B_1^*}{1 - \exp(-Le x_{1f_1})}, \quad (45a, b)$$

$x_{1f_1}$  is the initial non-dimensionalized stand-off distance, and  $B_1^*$  is the adiabatic heat-release parameter ( $\equiv 1 - T_{01}$ ).

Downstream at  $x_1 = \infty$  the boundary conditions are simply that  $T_u$ ,  $C_{\ell u}$ ,  $U_u$ ,  $V_u$  and  $p_u$  all decay to zero. Thus the linearized unsteady problem is now formulated for two dimensions with full allowance made for gas expansion. We now proceed to the analysis of this equation set, using first the fact that activation energy is large, and then approximating to the dispersion relation for small wavenumber.

### 3. Asymptotic analysis for large $\theta_1$

Equations (33)–(37) are now analysed in three zones: preheat ( $x_1 < x_{1f_1}$ ), equilibrium ( $x_1 > x_{1f_1}$ ) and reaction ( $x_1$  near  $x_{1f_1}$ ), where  $x_{1f_1}$  is the initial (steady) value of flame position. The analysis is very similar to that of I with some extensions to include series expansions for  $p$ ,  $u$  and  $v$ . These are summarized in Appendix B. Notice that the inner expansions are *not* the same as those obtained with  $\epsilon \gg \theta_1^{-1}$ . In this case ( $\epsilon \ll \theta_1^{-1}$ )  $T_u$ ,  $C_{\ell u}$ ,  $U_u$  and  $p_u$  are discontinuous to  $O(1)$  across the flame.

Using subscript 'p' to denote preheat zone, 'e' to denote equilibrium zone and an asterisk to mean 'evaluated at the flame (i.e.  $x_1 = x_{1f_1}$ )', we obtain the following jump conditions across the flame:

$$\overline{C_{\ell up}^*} + \frac{1}{Le} T_{up}^* = \frac{1}{Le} T_{ue}^*, \quad (46)$$

$$\frac{1}{Le B_1} \frac{dT_{up}}{dx_1} \Big|_{r_1} = \frac{1}{B_1} T_{up}^* + \frac{1}{2} \theta_1 T_{ue}^*, \quad (47)$$

$$(\overline{C_{\ell up}^*} + T_{up}^*) - \left( \frac{d\overline{C_{\ell up}}}{dx_1} \Big|_{r_1} + \frac{1}{Le} \frac{dT_{up}}{dx_1} \Big|_{r_1} \right) = \left( T_{ue}^* - \frac{1}{Le} \frac{dT_{ue}}{dx_1} \Big|_{r_1} \right), \quad (48)$$

$$U_{up}^* - U_{ue}^* = \frac{1}{T_{01}} (T_{up}^* - T_{ue}^*), \quad (49)$$

$$\frac{dV_{up}}{dx_1} \Big|_{r_1} - \frac{dV_{ue}}{dx_1} \Big|_{r_1} = \frac{1}{T_{01}^2} [Le B_1 H_u^* + ik(T_{up}^* - T_{ue}^*)], \quad (50)$$

$$(U_{up}^* - U_{ue}^*) + \frac{1}{\gamma} (p_{up}^* - p_{ue}^*) = \frac{4}{3} Sc \left( \frac{dU_{up}}{dx_1} \Big|_{r_1} - \frac{dU_{ue}}{dx_1} \Big|_{r_1} \right), \quad (51)$$

with

$$V_{up}^* = V_{ue}^*, \quad H_{up}^* = H_{ue}^*, \quad W_{up}^* = W_{ue}^*. \quad (52a, b, c)$$



Note that an overbar has been used above  $C_{\ell\text{up}}$  and  $dC_{\ell\text{up}}/dx_1$  to denote 'times  $(1+\sigma)Q_1/\sigma$ '.

The jump conditions (46)–(51) are equivalent to finding the jump conditions for each set of coefficient functions in the  $\theta_1^{-1}$  expansion and then reconstructing the series. In I for one dimension it was shown that near unit Lewis number the flame response was correctly predicted by a 'composite' dispersion relation obtained by reconstructing the asymptotic series in  $\theta_1^{-1}$ . Effectively this verified the method of setting up jump conditions at the beginning of the analysis, and thus this method has been adopted here.

The equations and boundary conditions in the preheat and equilibrium zones become as follows.

*Preheat:*

$$\omega T_{\text{up}} + \frac{dT_{\text{up}}}{dx_1} - (W_{\text{up}} - U_{\text{up}}(0)) \frac{dT_{\text{sp}}}{dx_1} - T_{01} \frac{dU_{\text{up}}}{dx_1} - ik V_{\text{up}} T_{\text{sp}} = 0, \quad (53)$$

$$\omega T_{\text{up}} + \frac{dT_{\text{up}}}{dx_1} - \frac{1}{Le} \frac{d^2 T_{\text{up}}}{dx_1^2} - (W_{\text{up}} - U_{\text{up}}(0)) \frac{dT_{\text{sp}}}{dx_1} - \frac{T_{\text{sp}}^2}{Le T_{01}^2} \left( ik \frac{dT_{\text{sp}}}{dx_1} H_{\text{up}} - k^2 T_{\text{up}} \right) = 0, \quad (54)$$

$$\omega \overline{C_{\ell\text{up}}} + \frac{d\overline{C_{\ell\text{up}}}}{dx_1} - \frac{d^2 \overline{C_{\ell\text{up}}}}{dx_1^2} - (W_{\text{up}} - U_{\text{up}}(0)) \frac{d\overline{C_{\ell\text{sp}}}}{dx_1} - \frac{T_{\text{sp}}^2}{T_{01}^2} \left( ik \frac{d\overline{C_{\ell\text{sp}}}}{dx_1} H_{\text{up}} - k^2 \overline{C_{\ell\text{up}}} \right) = 0, \quad (55)$$

$$\begin{aligned} \omega U_{\text{up}} + \frac{dU_{\text{up}}}{dx_1} + \frac{1}{\gamma} \frac{dp_{\text{up}}}{dx_1} - \frac{1}{T_{01}} (W_{\text{up}} - U_{\text{up}}(0)) \frac{dT_{\text{sp}}}{dx_1} \\ = \frac{4}{3} Sc \frac{d^2 U_{\text{up}}}{dx_1^2} - \frac{2}{3} \frac{Sc ik}{T_{01}} \frac{d}{dx_1} (T_{\text{sp}} V_{\text{up}}) + \frac{ik Sc}{T_{01}} T_{\text{sp}} \frac{dV_{\text{up}}}{dx_1} \\ + \frac{Sc T_{\text{sp}}^2}{T_{01}^2} \left( \frac{ik}{T_{01}} \frac{dT_{\text{sp}}}{dx_1} H_{\text{up}} - k^2 U_{\text{up}} \right), \end{aligned} \quad (56)$$

$$\begin{aligned} \omega V_{\text{up}} + \frac{dV_{\text{up}}}{dx_1} + \frac{ik T_{\text{sp}}}{\gamma T_{01}} p_{\text{up}} + \frac{Sc T_{\text{sp}} H_{\text{up}}}{T_{01}^2} \frac{d^2 T_{\text{sp}}}{dx_1^2} - \frac{T_{\text{sp}} H_{\text{up}}}{T_{01}^2} \frac{dT_{\text{sp}}}{dx_1} - \frac{T_{\text{sp}} H_{\text{up}} g r}{T_{01}} \\ = Sc \frac{d^2 V_{\text{up}}}{dx_1^2} - \frac{4}{3} \frac{k^2 Sc}{T_{01}^2} T_{\text{sp}}^2 V_{\text{up}} + \frac{ik Sc}{T_{01}} \frac{dT_{\text{sp}}}{dx_1} U_{\text{up}} \\ + \frac{Sc}{T_{01}^2} \frac{dT_{\text{sp}}}{dx_1} \frac{d}{dx_1} (T_{\text{sp}} H_{\text{up}}) + \frac{1}{3} \frac{ik Sc}{T_{01}} T_{\text{sp}} \frac{dU_{\text{up}}}{dx_1}, \end{aligned} \quad (57)$$

$$\text{where} \quad H_{\text{up}} T_{\text{sp}} = -ik \int_0^{x_1} T_{\text{up}} dx_1, \quad (58)$$

$$W_{\text{up}} = ik \int_0^{x_1} V_{\text{up}} dx_1, \quad (59)$$

$$\text{with} \quad T_{\text{up}}(0) = 0, \quad (60)$$

$$\overline{C_{\ell\text{up}}}(0) - \frac{d\overline{C_{\ell\text{up}}}}{dx_1} \Big|_0 = -k\Omega_3 \frac{p_{\text{up}}(0)}{\gamma} B_1 \exp(-x_{1f}), \quad (61)$$

$$U_{\text{up}}(0) = -k\Omega_3 \frac{p_{\text{up}}(0)}{\gamma}, \quad (62)$$

$$V_{\text{up}}(0) = -ik\Omega_2 \frac{p_{\text{up}}(0)}{\gamma}, \quad (63)$$

and, from the steady solutions,

$$T_{\text{sp}} = 1 - B_1 + B_1 \exp [Le(x_1 - x_{1f_1})], \quad (64)$$

$$\overline{C_{\ell\text{sp}}} = -B_1[\exp(x_1 - x_{1f_1}) - 1]. \quad (65)$$

*Equilibrium:*

$$\omega T_{\text{ue}} + \frac{dT_{\text{ue}}}{dx_1} - T_{01} \frac{dU_{\text{ue}}}{dx_1} - ikV_{\text{ue}} = 0, \quad (66)$$

$$\left(\omega + \frac{k^2}{Le T_{01}^2}\right) T_{\text{ue}} + \frac{dT_{\text{ue}}}{dx_1} - \frac{1}{Le} \frac{d^2 T_{\text{ue}}}{dx_1^2} = 0, \quad (67)$$

$$\omega U_{\text{ue}} + \frac{dU_{\text{ue}}}{dx_1} + \frac{1}{\gamma} \frac{dp_{\text{ue}}}{dx_1} = \frac{4}{3} Sc \frac{d^2 U_{\text{ue}}}{dx_1^2} + \frac{1}{3} \frac{ik Sc}{T_{01}} \frac{dV_{\text{ue}}}{dx_1} - \frac{Sc k^2}{T_{01}^2} U_{\text{ue}}, \quad (68)$$

$$\omega V_{\text{ue}} + \frac{dV_{\text{ue}}}{dx_1} - Sc \frac{d^2 V_{\text{ue}}}{dx_1^2} = \frac{H_{\text{ue}} g_r}{T_{01}} - \frac{ik p_{\text{ue}}}{\gamma T_{01}} - \frac{4 k^2 Sc}{3 T_{01}^2} V_{\text{ue}} + \frac{1}{3} \frac{ik Sc}{T_{01}} \frac{dU_{\text{ue}}}{dx_1}, \quad (69)$$

$$H_{\text{ue}} = H_{\text{ue}}^* - ik \int_{x_{1f_1}}^{x_1} T_{\text{ue}} dx_1, \quad (70)$$

$$W_{\text{ue}} = W_{\text{ue}}^* + ik \int_{x_{1f_1}}^{x_1} V_{\text{ue}} dx_1, \quad (71)$$

$$\overline{C_{\ell\text{ue}}} = 0, \quad (72)$$

with  $T_{\text{ue}}(\infty) = 0$ ;  $U_{\text{ue}}(\infty) = 0$ ;  $V_{\text{ue}}(\infty) = 0$ ;  $p_{\text{ue}}(\infty) = 0$ , (73a, b, c, d)

$$T_{\text{se}} = 1; \quad C_{\ell\text{se}} = 0. \quad (74a, b)$$

Because of the intractable nature of the preheat equations, it is not possible to obtain an exact analytical solution to the differential equations (53)–(57) and then proceed with equations (66)–(69) and conditions (46)–(52), (60)–(63), (73) to obtain an exact form for the dispersion relation between  $\omega$  and  $k$ . Only by assuming a ‘constant-density’ approach (whereby all terms explicit in  $T_{\text{sp}}$  and  $dT_{\text{sp}}/dx_1$  in (53)–(57) are replaced by 1, 0 respectively) can an exact solution be found. This somewhat-artificial route has been worked through by a number of authors, and in our terminology the two-dimensional version of equation (150) of I with zero gas expansion is given by

$$\frac{k^2}{Le^2} (Le - 1) + (s_1^2 - \frac{1}{2}S + \frac{1}{2}R - RS) + \frac{2[1 - \exp(-Le x_{1f_1})]}{B_1^* \theta_1} (\frac{1}{2} + R) (\frac{1}{2} - S) (s + S) = 0, \quad (75)$$

where

$$r_1 \equiv (\omega + k^2 + \frac{1}{4})^{\frac{1}{2}}, \quad (76)$$

$$s_1 \equiv \left(\frac{\omega}{Le} + \frac{k^2}{Le^2} + \frac{1}{4}\right)^{\frac{1}{2}}, \quad (77)$$

$$R \equiv r_1 \frac{\cosh(r_1 x_{1f_1})}{\sinh(r_1 x_{1f_1})}, \quad (78)$$

$$S \equiv s_1 \frac{\cosh(Le s_1 x_{1f_1})}{\sinh(Le s_1 x_{1f_1})}. \quad (79)$$

Notice that only the terms explicitly dependent on  $T_{\text{sp}}$  in (53)–(57) have  $T_{\text{sp}}$  set to 1 ( $B_1^* = 0$ ) to simulate zero gas expansion. The  $B_1^* \theta_1$  term remains unaltered, being the product of heat release and activation energy and directly equivalent to the reduced activation energy  $\beta$  of Peleé & Clavin (1982).

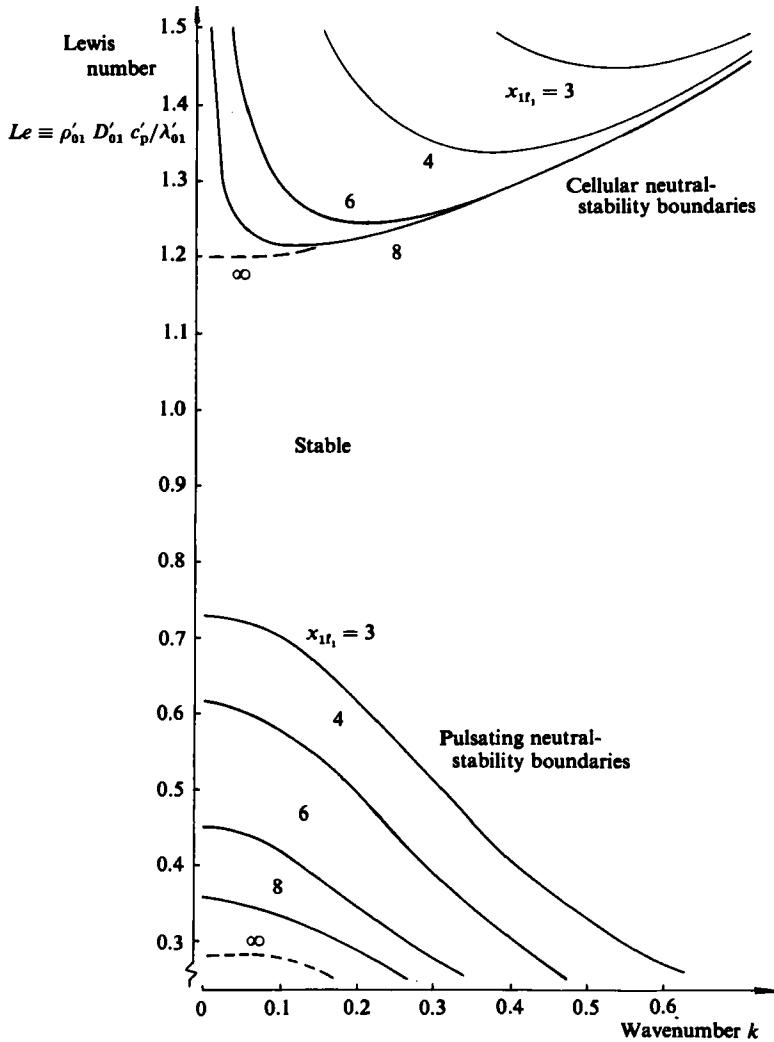


FIGURE 2. Two-dimensional neutral-stability boundaries with zero gas expansion (i.e.  $\rho' = \text{const.}$ ), activation energy  $\theta_1 B_1^* = 10$ . Stable response predicted within region enclosed by two curves for each  $x_{1f_1}$ .

The relation (75) is similar to that derived by Buckmaster (1983) and (for one-dimension) to that obtained by Margolis (1980). It is a useful comparison for the approximate theories, which are now developed to solve the preheat equations for non-zero gas expansion. Before proceeding to this, we summarize some of the main conclusions from the analysis of this result.

The neutral-stability curves resulting from relation (75) are set out in figure 2 for a typical value of  $\theta_1 B_1^* = 10$ . It is now known that the cellular instability ( $Le < 1$ ) is suppressed as the heat loss to the holder is increased (Buckmaster 1983). On the other hand, in general the pulsating instability ( $Le < 1$ ) is made more accessible when there is heat loss to the holder present. In the work of McIntosh & Clarke (1983) leading-order theory alone was used, and it was shown that the planar ( $k = 0$ ) neutral-stability curve reaches a maximum near  $x_{1f_1} = 2$  such that to either side of this  $x_{1f_1}$  value, the effect of the holder is to suppress instability. This trend is confirmed

by the more accurate predictions of second-order theory (see I, figure 4) and in independent work by Buckmaster (1983). In both these latter papers it is predicted that the Lewis number for the turning point becomes closer to unity as  $\theta_1 B_1^*$  increases, till for very large  $\theta_1 B_1^*$ , the turning point occurs for  $Le > 1$  (rather than  $Le < 1$  for moderate values of  $\theta_1 B_1^*$  - note that Lewis number in the Buckmaster paper is the inverse of that used here). As one would expect for  $\theta_1 B_1^*$  increased still further (see e.g. the  $\theta_1 B_1^* = 50$  curve of figure 5 of Buckmaster (1983) and figure 2 of McIntosh & Clarke (1983)), the neutral-stability curve for leading-order theory alone is recovered. As Buckmaster points out, this curve will be more relevant for 'limit' mixtures (i.e. when flame speeds are low) since activation energies will be very large owing to low flame temperatures. One cautionary remark should be made concerning the nature of the neutral stability curve for small  $x_{1f_1}$ . As pointed out in I, the high frequencies of pulsation predicted below the  $x_{1f_1}$  turning value tend to suggest that time should be rescaled to take account of very fast flame response. Hence in that paper the curves were dotted in this region, indicating that the predictions of the theory may need further verification by experiments and better modelling techniques.

Returning to the main problem of solving the differential equations for non-zero gas expansion, we observe that the equilibrium-zone equations do have an exact solution given by

$$T_{ue} = T_{ue}^* \exp[Le(\frac{1}{2}-s)(x_1 - x_{1f_1})], \quad (80)$$

$$\frac{p_{ue}}{\gamma} = \frac{p_{ue}^{**}}{\gamma} \exp\left[-\frac{k}{T_{01}}(x_1 - x_{1f_1})\right] - i \frac{H_{ue}^{**}}{k} g_r + \Theta_3 T_{ue}^* \exp[Le(\frac{1}{2}-s)(x_1 - x_{1f_1})], \quad (81)$$

$$U_{ue} = U_{ue}^{**} \exp\left[\frac{1}{Sc}(\frac{1}{2}-a)(x_1 - x_{1f_1})\right] + \frac{k p_{ue}^{**}}{\gamma T_{01}(\omega - k/T_{01})} \exp\left[-\frac{k}{T_{01}}(x_1 - x_{1f_1})\right] + \Theta_5 T_{ue}^* \exp[Le(\frac{1}{2}-s)(x_1 - x_{1f_1})], \quad (82)$$

$$V_{ue} = \frac{1}{ik} \left\{ -\frac{T_{01}}{Sc}(\frac{1}{2}-a) U_{ue}^{**} \exp\left[\frac{1}{Sc}(\frac{1}{2}-a)(x_1 - x_{1f_1})\right] + \frac{k^2 p_{ue}^{**}}{\gamma T_{01}(\omega - k/T_{01})} \times \exp\left[-\frac{k}{T_{01}}(x_1 - x_{1f_1})\right] + \Theta_6 T_{ue}^* \exp[Le(\frac{1}{2}-s)(x_1 - x_{1f_1})\right] \right\}, \quad (83)^\dagger$$

where

$$\Theta_1 \equiv \left[ -\frac{\omega}{T_{01}} \left( \omega + \frac{k^2 Sc}{T_{01}^2} \right) - Le(\frac{1}{2}-s) \left( \frac{2\omega}{T_{01}} + (1+\omega) \frac{k^2 Sc}{T_{01}^3} \right) + Le^2(\frac{1}{2}-s)^2 \left( \frac{Sc}{T_{01}} \left( \omega - \frac{k^2}{T_{01}^2} \right) - \frac{1}{T_{01}} \right) + \frac{Le^3(\frac{1}{2}-s)^3 Sc}{T_{01}} + \frac{k^2 g_r}{T_{01}^2 Le(\frac{1}{2}-s)} \right], \quad (84)$$

$$\Theta_2 \equiv \Theta_1 + \frac{1}{3} \frac{Sc}{T_{01}} (\omega Le^2(\frac{1}{2}-s)^2 + Le^3(\frac{1}{2}-s)^3), \quad (85)$$

† Downstream where temperature fluctuations are negligible, one has the Euler equations in pressure and the two components of velocity. The apparent singularity of (83) when  $k = 0$  arises from the continuity equation (66). This reads

$$\frac{dU_{ue}}{dx_1} = -\frac{ik}{T_{01}} V_{ue},$$

so that for  $k = 0$  one requires a zero-gradient condition on  $U_{ue}$  downstream. The other apparent singularity when  $\omega = k/T_{01}$  can only occur when  $\omega$  is real and positive (since  $k$  is real and positive). Thus the singularity takes place in a region already unstable, and thus will not be of significance in this theory.

$$\Theta_3 \equiv \frac{\Theta_2}{Le^2 (\frac{1}{2}-s)^2 - k^2/T_{01}^2}, \quad (86)$$

$$\Theta_4 \equiv -Le (\frac{1}{2}-s) \Theta_3 + \frac{1}{3} \frac{Sc}{T_{01}} (\omega Le (\frac{1}{2}-s) + Le^2 (\frac{1}{2}-s)^2), \quad (87)$$

$$\Theta_5 \equiv \frac{\Theta_4}{\omega + k^2 Sc/T_{01}^2 + Le (\frac{1}{2}-s) - Sc Le^2 (\frac{1}{2}-s)^2}, \quad (88)$$

$$\Theta_6 \equiv \omega + Le (\frac{1}{2}-s) - T_{01} Le (\frac{1}{2}-s) \Theta_5, \quad (89)$$

$$\frac{p_{ue}^{**}}{\gamma} \equiv \frac{p_{ue}^*}{\gamma} - \Theta_3 T_{ue}^* + i \frac{H_{ue}^{**}}{k} g_r, \quad (90)$$

$$U_{ue}^{**} \equiv U_{ue}^* - \frac{k p_{ue}^{**}}{\gamma T_{01} (\omega - k/T_{01})} - \Theta_5 T_{ue}^*, \quad (91)$$

$$H_{ue}^{**} \equiv H_{ue}^* + \frac{ik T_{ue}^*}{Le (\frac{1}{2}-s)}, \quad (92)$$

$$H_{ue}^* \equiv -ik \int_0^{x_{f1}} T_{up} dx_1 = H_{up}^*, \quad (93)$$

and where

$$s \equiv \left( \frac{\omega}{Le} + \frac{k^2}{Le^2 T_{01}^2} + \frac{1}{4} \right)^{\frac{1}{2}}, \quad (94)$$

$$a \equiv \left( Sc \omega + \frac{k^2 Sc^2}{T_{01}^2} + \frac{1}{4} \right)^{\frac{1}{2}}. \quad (95)$$

This solution to the equilibrium equations is essentially that obtained by Pelcé & Clavin (1982), but with the inclusion of the (small) effect of the downstream temperature field. This latter is included, since the solution is required immediately downstream of the flame and not just at distances of the order of the so-called 'hydrodynamic zone'.

We now turn to approximate small-wavenumber analysis to solve the preheat equations for non-zero gas expansion.

#### 4. Small-wavenumber analysis

In order to solve (53)–(57) we make the approximation that wavenumber is small. The problem immediately becomes more manageable if one also assumes that the complex frequency  $\omega$  is small. Thus, specifically, if  $\delta$  is regarded as a small number, we write

$$k = T_{01} \bar{k} \delta, \quad \omega = \bar{\omega} \delta. \quad (96), (97)$$

Since, for pulsating flames,  $\omega$  is not always small, one must recognize that the theory will not necessarily have validity for such modes. However for cellular flames, the approximation (97) will hold true near the neutral stability boundary.

The preheat equations (53)–(57) then degenerate to a series of second-order differential equations with constant coefficients and progressively more complicated forcing terms as order  $\delta$  and order  $\delta^2$  terms are included. We write

$$X_{up} = X_{up0} + \delta X_{up1} + \delta^2 X_{up2} \dots \quad [X = T, C_r, u, v, p]. \quad (98a)$$

$$Y_{ue} = Y_{ue0} + \delta Y_{ue1} + \delta^2 Y_{ue2} \dots \quad [Y = T, u, v, p]. \quad (98b)$$

It can be shown from (52a) and (57), with (63), (73c) and (96), that the transverse velocity throughout is  $O(\delta)$ , so that

$$V_{\text{up}0} = V_{\text{ue}0} = 0, \quad (99a, b)$$

and the equations become as follows.

*Preheat  $O(1)$ :*

$$\frac{dT_{\text{up}0}}{dx_1} - T_{01} \frac{dU_{\text{up}0}}{dx_1} = 0, \quad (100)$$

$$\frac{dT_{\text{up}0}}{dx_1} - \frac{1}{Le} \frac{d^2T_{\text{up}0}}{dx_1^2} = 0, \quad (101)$$

$$\frac{d\overline{C_{\ell\text{up}0}}}{dx_1} - \frac{d^2\overline{C_{\ell\text{up}0}}}{dx_1^2} = 0, \quad (102)$$

$$\frac{dU_{\text{up}0}}{dx_1} + \frac{1}{\gamma} \frac{dp_{\text{up}0}}{dx_1} - \frac{4}{3} Sc \frac{d^2U_{\text{up}0}}{dx_1^2} = 0. \quad (103)$$

*Preheat  $O(\delta)$ :*

$$\frac{dT_{\text{up}1}}{dx_1} - T_{01} \frac{dU_{\text{up}1}}{dx_1} = -\bar{\omega} T_{\text{up}0} + T_{01} \bar{\kappa} \Omega_3 \frac{p_{\text{up}0}(0)}{\gamma} \frac{dT_{\text{sp}}}{dx_1}, \quad (104)$$

$$\frac{dT_{\text{up}1}}{dx_1} - \frac{1}{Le} \frac{d^2T_{\text{up}1}}{dx_1^2} = -\bar{\omega} T_{\text{up}0} + T_{01} \bar{\kappa} \Omega_3 \frac{p_{\text{up}0}(0)}{\gamma} \frac{dT_{\text{sp}}}{dx_1}, \quad (105)$$

$$\frac{d\overline{C_{\ell\text{up}1}}}{dx_1} - \frac{d^2\overline{C_{\ell\text{up}1}}}{dx_1^2} = -\bar{\omega} \overline{C_{\ell\text{up}0}} + T_{01} \bar{\kappa} \Omega_3 \frac{p_{\text{up}0}(0)}{\gamma} \frac{d\overline{C_{\ell\text{sp}}}}{dx_1}, \quad (106)$$

$$\frac{dU_{\text{up}1}}{dx_1} + \frac{1}{\gamma} \frac{dp_{\text{up}1}}{dx_1} - \frac{4}{3} Sc \frac{d^2U_{\text{up}1}}{dx_1^2} = -\bar{\omega} U_{\text{up}0} + T_{01} \bar{\kappa} \Omega_3 \frac{p_{\text{up}0}(0)}{\gamma} \frac{dT_{\text{sp}}}{dx_1}, \quad (107)$$

$$\begin{aligned} \frac{dV_{\text{up}1}}{dx_1} - Sc \frac{d^2V_{\text{up}1}}{dx_1^2} &= -\frac{i\bar{\kappa}}{\gamma} T_{\text{sp}} p_{\text{up}0} - Sc \frac{T_{\text{sp}} H_{\text{up}1}}{T_{01}^2} \frac{d^2T_{\text{sp}}}{dx_1^2} \\ &+ \frac{T_{\text{sp}} H_{\text{up}1}}{T_{01}^2} \frac{dT_{\text{sp}}}{dx_1} + \frac{T_{\text{sp}} H_{\text{up}1}}{T_{01}} g_r + i\bar{\kappa} Sc \frac{dT_{\text{sp}}}{dx_1} U_{\text{up}0} \\ &+ \frac{Sc}{T_{01}^2} \frac{dT_{\text{sp}}}{dx_1} \frac{d}{dx_1} (T_{\text{sp}} H_{\text{up}1}) + \frac{4}{3} i\bar{\kappa} Sc T_{\text{sp}} \frac{dU_{\text{up}0}}{dx_1}, \end{aligned} \quad (108)$$

$$\frac{1}{T_{01}} \frac{d}{dx_1} (H_{\text{up}1} T_{\text{sp}}) = -i\bar{\kappa} T_{\text{up}0}. \quad (109)$$

*Preheat  $O(\delta^2)$ :*

$$\begin{aligned} \frac{dT_{\text{up}2}}{dx_1} - \frac{1}{Le} \frac{d^2T_{\text{up}2}}{dx_1^2} &= -\bar{\omega} T_{\text{up}1} + W_{\text{up}2} \frac{dT_{\text{sp}}}{dx_1} \\ &+ \frac{T_{\text{sp}}^2}{Le} \left[ \frac{i\bar{\kappa}}{T_{01}} \frac{dT_{\text{sp}}}{dx_1} H_{\text{up}1} - \bar{\kappa}^2 T_{\text{up}0} \right] + T_{01} \bar{\kappa} \Omega_3 \frac{p_{\text{up}1}(0)}{\gamma} \frac{dT_{\text{sp}}}{dx_1}, \end{aligned} \quad (110)$$

$$\frac{d\overline{C_{\ell_{up2}}}}{dx_1} - \frac{d^2\overline{C_{\ell_{up2}}}}{dx_1^2} = -\overline{\omega C_{\ell_{up1}}} + W_{up2} \frac{d\overline{C_{\ell_{sp}}}}{dx_1} + T_{sp}^2 \left[ \frac{i\bar{\kappa}}{T_{01}} \frac{d\overline{C_{\ell_{sp}}}}{dx_1} H_{up1} - \bar{\kappa}^2 C_{\ell_{up0}} \right] + T_{01} \bar{\kappa} \Omega_3 \frac{p_{up1}(0)}{\gamma} \frac{d\overline{C_{\ell_{sp}}}}{dx_1}, \quad (111)$$

$$\frac{1}{T_{01}} \frac{dW_{up2}}{dx_1} = i\bar{\kappa} V_{up1}. \quad (112)$$

*Equilibrium zone:*

it can be shown that the solution of the equilibrium equations for small  $\omega$  and  $k$  is given by

$$T_{ue} = T_{ue0}^* + \delta [T_{ue1}^* - \overline{\omega} T_{ue0}^*(x_1 - x_{1f_1})] + \delta^2 \left[ T_{ue2}^* - \overline{\omega} T_{ue1}^*(x_1 - x_{1f_1}) + \frac{1}{Le} T_{ue0}^* \bar{z}(x_1 x_{1f_1}) + \frac{1}{2} T_{ue0}^* \overline{\omega}^2 (x_1 - x_{1f_1})^2 \right] + \dots, \quad (113)$$

$$\frac{p_{ue}}{\gamma} = \frac{p_{ue0}^*}{\gamma} + \delta \left[ \frac{p_{ue1}^*}{\gamma} - \overline{\omega} U_{ue0}^*(x_1 - x_{1f_1}) \right] + O(\delta^2), \quad (114)$$

$$U_{ue} = U_{ue0}^* + \delta U_{ue1}^* + O(\delta^2), \quad (115)$$

$$V_{ue} = \frac{\delta}{i\bar{\kappa}} \left[ \overline{\omega} U_{ue1}^* - \frac{\bar{\kappa} p_{ue1}^*}{\gamma} + \frac{\bar{z} T_{ue0}^*}{T_{01} Le} - \frac{i H_{ue2}^*}{T_{01}} g_r - (1 - Sc) g_r \bar{\kappa}^2 T_{ue0}^*(x_1 - x_{1f_1}) + Sc \bar{\kappa} U_{ue0}^*(\overline{\omega} + \bar{\kappa}) + \overline{\omega} \bar{\kappa} U_{ue0}^*(x_x - x_{1f_1}) \right] + O(\delta^2), \quad (116)$$

where

$$H_{ue1}^* \equiv -iT_{01} \bar{\kappa} \int_0^{x_{1f_1}} T_{up1} dx_1, \quad (117)$$

$$H_{ue2}^* \equiv -iT_{01} \bar{\kappa} \int_0^{x_{1f_1}} T_{up2} dx_1, \quad (118)$$

$$\bar{z} \equiv \overline{\omega}^2 - \bar{\kappa}^2, \quad (119)$$

$$\frac{p_{ue0}^*}{\gamma} = \frac{\overline{\omega}}{\bar{\kappa}} U_{ue0}^* - \frac{i H_{ue1}^*}{\bar{\kappa} T_{01}} g_r, \quad (120)$$

and it has been recognized that in order to obtain the dispersion relation to  $\delta^2$  accuracy, only  $T_u$  and  $C_{\ell_u}$  are required to  $O(\delta^2)$ .

The boundary conditions are exactly the same form as (60)–(63), (73a–d) with the relevant coefficient functions of the expansions (98a, b) inserted. The jump conditions (46)–(52) also follow through at each order in  $\delta$ , in exactly the same manner.

The solution to the whole problem is now a matter of solving the differential equations in the preheat zone at each order in  $\delta$ . This somewhat-tedious process is not detailed here. The method involves the solution of (108) for  $V_{up1}$ , which is then integrated to give  $W_{up2}$  (see (112)). These solutions are then substituted into the right-hand side of (110) and (111) in  $T_{up2}$ ,  $\overline{C_{\ell_{up2}}}$ . This process of solving for temperature and lean species uses all boundary conditions and jump conditions except for (48). At this juncture all the solutions are in terms of  $T_{up0}^*$ ,  $T_{up1}^*$ ,  $T_{up2}^*$ . The insertion of these solutions into (48) then results in a solvability condition that is a dispersion relation between  $\overline{\omega}$  and  $\bar{\kappa}$ . It is found that this condition is of the form

$$F_0 + \delta F_1 \overline{\omega} + \delta F_2 \bar{\kappa} + \delta^2 F_3 \overline{\omega}^2 + \delta^2 F_4 \overline{\omega} \bar{\kappa} + \delta^2 F_5 \bar{\kappa}^2 = 0, \quad (121)$$

where the constants  $F_0, \dots, F_5$  are functions of  $Le, x_{1f_1}, T_{01}, Pr, \theta_1 B_1^*, g_r, \Omega_1$  and  $\Omega_2$ , and are listed in McIntosh (1984). Condition (121), rewritten in terms of  $\omega$  and  $k$ , is in fact a quadratic in  $\omega$ ;

$$A(k)\omega^2 + B(k)\omega + C(k) = 0, \quad (122)$$

where

$$A(k) \equiv F_3, \quad (123)$$

$$B(k) \equiv F_1 + \frac{F_4 k}{T_{01}}, \quad (124)$$

$$C(k) \equiv F_0 + F_2 \frac{k}{T_{01}} + F_5 \frac{k^2}{T_{01}^2}. \quad (125)$$

The result (122) can now be used as a basis for discussing the stability of burner flames subject to two-dimensional infinitesimal disturbances, where gas expansion is fully allowed for, and the influences of the flameholder and gravitational acceleration are included.

The constants  $F_1, \dots, F_5$  are in general complicated functions of the parameters mentioned above. However, the important constant  $F_0$  reduces simply to

$$F_0 = -\left(\frac{1}{\exp(Le x_{1f_1}) - 1}\right) \left(1 + \frac{2}{\theta_1 B_1}\right), \quad (126)$$

and immediately highlights the order of  $x_{1f_1}$  (stand-off distance) for the expansion (121) to be valid. As  $\delta \rightarrow 0$ , so  $F_0$  must vanish, which implies that

$$Le x_{1f_1} = O\left(\ln \frac{1}{\delta}\right). \quad (127)$$

This restriction is quite permissible in the context of the burner problem we are addressing. It amounts to a restriction of small heat loss to the burner. It will be seen from §5 that an acceptable upper limit for  $k$  is about 0.2. Thus if  $\delta \sim 0.2$ , then  $Le x_{1f_1}$  can be as small as 1.6. If  $\delta \sim 0.1$ , which is certainly well within the accuracy of this theory, then  $Le x_{1f_1}$  is only barred from values below about 2.3. Thus the validity of the expansion (121) is easily maintained.

## 5. Discussion

In that condition (122) is an approximation to the dispersion relation for small  $\omega$  as well as small  $k$ , one must recognise that it cannot give very accurate results for the pulsating neutral-stability boundary. The reason for this becomes evident when we observe that the planar ( $k = 0$ ) analysis predicted  $\omega = i\hat{\omega}$  values along this line that were not particularly small ( $\hat{\omega} = 0.3-0.4$ , are typical values – see I and Buckmaster 1983). Thus the analysis will not reproduce precisely the results of the *exact* planar theory. One can thus only obtain a general indication of the effect of gas expansion on the condition for neutrally stable pulsations. The indications are that the shape of the curves in the lower part of figure 2 are not drastically altered by gas expansion. In that we are restricted to small  $k$  in this analysis, the *onset* of planar instability will be well predicted by the planar dispersion relation derived in I (equation (148)) and equivalent to (75) in this paper with  $k = 0$ . This point is referred to again at the end of this discussion.

If we now consider cellular flames, we note that the condition for neutral stability is that  $\omega = 0$ . This is the condition for a standing two-dimensional wave pattern to be observed (for a particular value of wavenumber  $k$ ). Thus the predictions of (122)



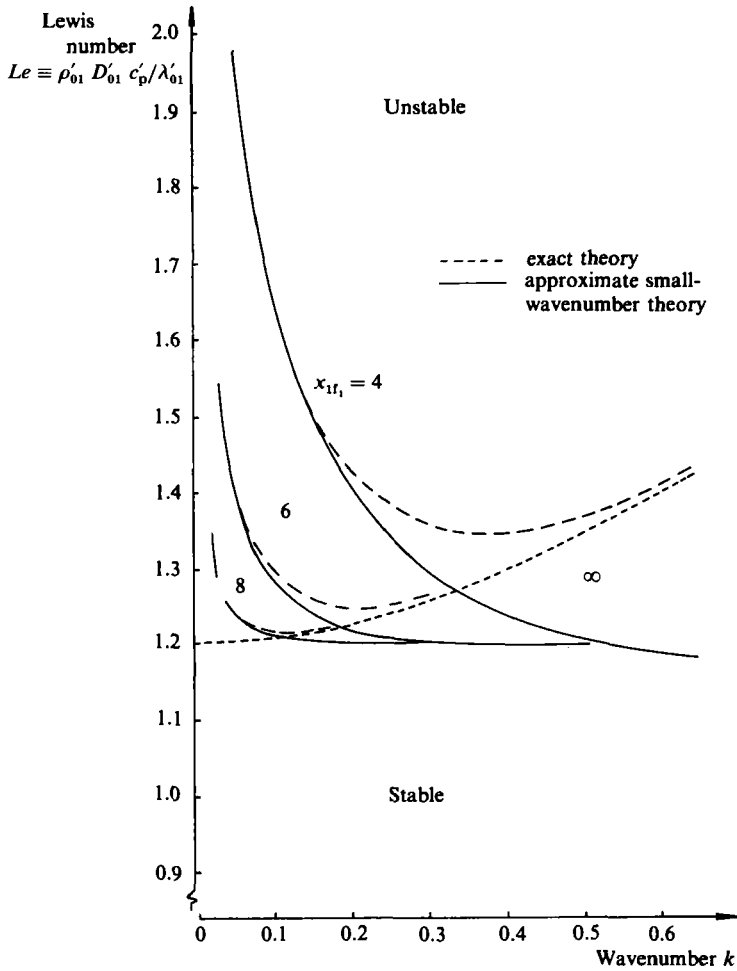


FIGURE 3. Test of small-wavenumber theory for zero gas expansion, activation energy  $\theta_1 B_1^* = 10$ , and for three stand-off distances  $x_{1r_1}$ . All curves related to upper cellular neutral-stability boundary below which stable conditions are predicted.

are accurate as long as  $k$  is small. The neutral-stability condition is simply  $C(k) = 0$ , i.e.

$$F_0 + F_2 \frac{k}{T_{01}} + F_5 \frac{k^2}{T_{01}^2} = 0. \tag{128}$$

As a check on this result, the neutral-stability curves resulting from (128) are compared with those obtained from the exact relationship (75) for zero gas expansion (that is with  $T_{01} = 1$ ) (see figure 3). Up to about  $k = 0.2$ , the curves follow closely the exact results. For larger  $k$ -values the loss of  $k^3$  and higher terms removes the minimum behaviour that the exact relationship predicts. Nevertheless, we have enough confidence in the approximate technique to show clearly the effect of gas expansion, gravity and the Darcy constants, for cellular flames with low wavenumber. In figure 4 the effect of gas expansion is displayed for  $\theta_1 B_1^* = 10$ ,  $x_{1r_1} = 4, 6, 8$ ,  $g_r = 0$ ,  $\Omega_1 = 0$  and  $Pr = 0.75$ . The unbroken lines are plots of critical Lewis number for neutral stability against wavenumber  $k$ , with  $T_{01} = 0.3$ . The broken lines are plots for  $T_{01} = 0.5$ . Typically,  $T_{01}$  will be in the region of 0.2–0.3, so that the main effect

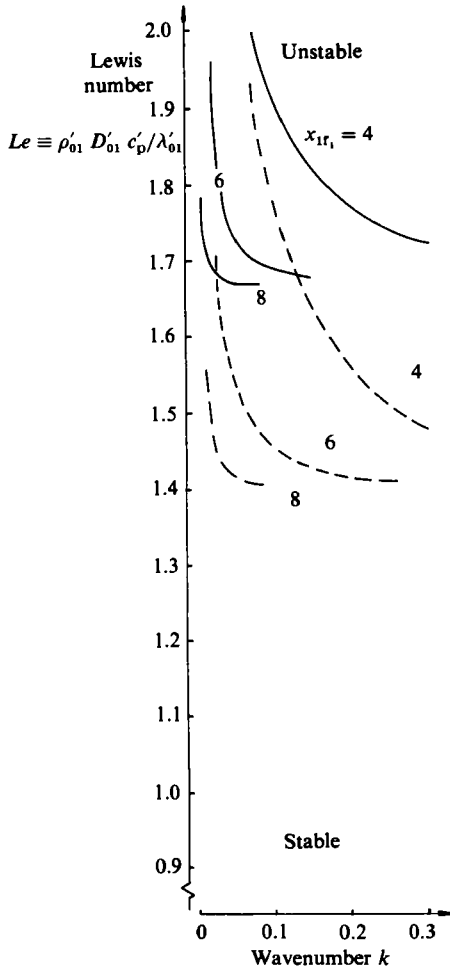


FIGURE 4

FIGURE 4. Effect of gas expansion on cellular neutral stability boundary;  $\theta_1 B_1^* = 10$ ,  $Pr = 0.75$  and for three  $x_{1f_1}$  values. —,  $T_{01} = 0.3$ ; ----, 0.5.

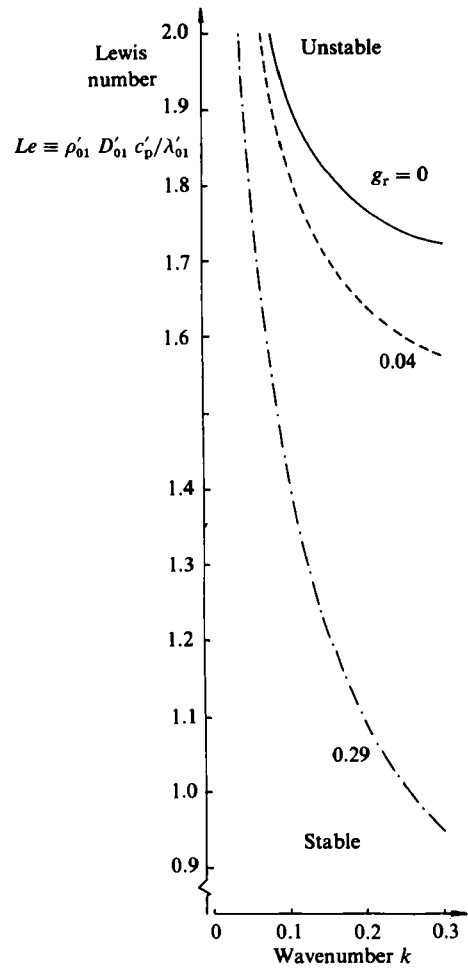


FIGURE 5

FIGURE 5. Effect of gravity on cellular neutral-stability boundary;  $\theta_1 B_1^* = 10$ ,  $Pr = 0.75$ ,  $x_{1f_1} = 4$ ,  $T_{01} = 0.3$ .

of gas expansion *on its own* is to suppress the cellular instability. This confirms the findings of other authors (see Clavin & Williams, 1982, p. 267).

In figure 5, the effect of gravity is displayed on the test curve  $\theta_1 B_1^* = 10$ ,  $x_{1f_1} = 4$ ,  $\Omega_1 = \Omega_2 = 0$ ,  $T_{01} = 0.3$ ,  $Pr = 0.75$ . The constant  $g_r$  defined by (10) is very sensitive to changes in inlet flow speed. Typical values for a diffusion coefficient of approximately  $D'_{01} = 0.3 \text{ cm}^2/\text{s}$  are  $g_r = 0.29$  for  $u'_{01} = 10 \text{ cm/s}$  and  $g_r = 0.04$  for  $u'_{01} = 20 \text{ cm/s}$ . Since  $g_r$  can vary quite considerably, we have considered it an  $O(1)$  parameter throughout this work, and its effect is clearly demonstrated in figure 5. The unbroken lines are neutral-stability curves for  $g_r = 0$ , the broken lines are plots for  $g_r = 0.04$  and the chained lines are plots for  $g_r = 0.29$ . Thus the main effect of the non-dimensional gravitational acceleration  $g_r$  on its own is to encourage the onset of cellular instability. However this is somewhat of an artificial exercise here, since in reality as  $u'_{01}$  decreases (and  $g_r$  increases),  $x_{1f_1}$  will generally *decrease*. Consequently

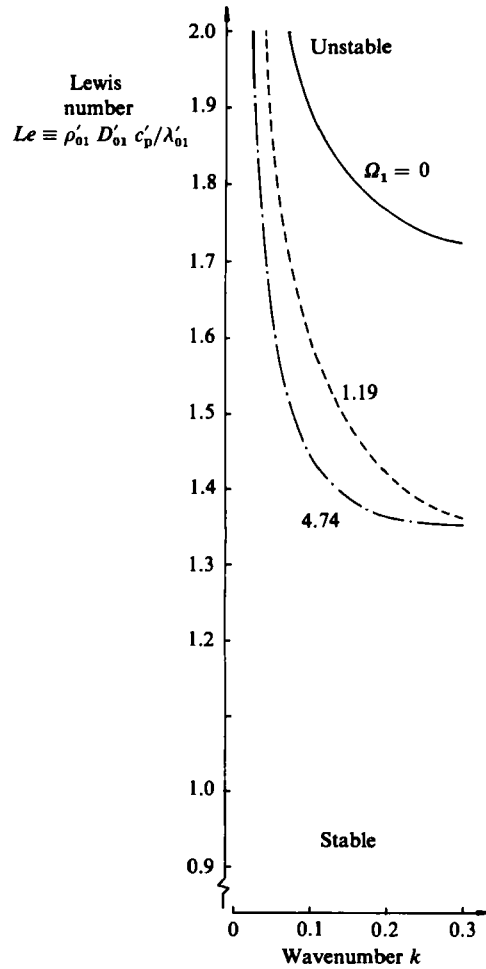


FIGURE 6. Effect of longitudinal Darcy constant  $\Omega_1$  on cellular neutral-stability boundary;  $\theta_1 B_1^* = 10$ ,  $Pr = 0.75$ ,  $x_{1f_1} = 4$ ,  $T_{01} = 0.3$ ,  $g_r = 0$ , porosity  $\beta = 0.75$ , transverse constant  $\Omega_2 = \Omega_1$ .

the true effect of buoyancy will be the competition of the two effects illustrated in figures 4 and 5.

In figure 6, the effect of the Darcy constant is shown on the test case  $\theta_1 B_1^* = 10$ ,  $x_{1f_1} = 4$ ,  $T_{01} = 0.3$ ,  $Pr = 0.75$ ,  $g_r = 0$ . From equation (18), one should realise that the non-dimensional constant  $\Omega_1$  increases with velocity  $u'_{01}$ , and for  $D'_{01} = 0.3 \text{ cm}^2/\text{s}$ , Lewis number near unity and  $Pr = 0.75$ , typical values are  $\Omega_1 = 1.19$  for  $U'_{01} = 10 \text{ cm/s}$  and  $\Omega_1 = 4.74$  for  $U'_{01} = 20 \text{ cm/s}$ . The destabilizing effect of  $\Omega_1$  is clearly seen in the dotted ( $\Omega_1 = 1.19$ ) and the chained ( $\Omega_1 = 4.74$ ) lines in figure 6, where a porosity of 0.75 has been assumed and the Darcy constant in the transverse direction ( $\Omega_2$ ) is assumed equal to  $\Omega_1$ .

Though not illustrated here, it should be noted that an increase in  $\theta_1 B_1^*$  tends also to draw the neutral-stability curves downwards (i.e. reduces  $Le_{crit}$ ), but that Prandtl-number changes have only a small effect.

In reality, the overall effect of gas expansion, gravity, activation energy and the Darcy constants will be quite complicated. As inlet speed increases,  $x_{1f_1}$  will increase and  $g_r$  will decrease. These two effects will be stabilizing for flames with Lewis

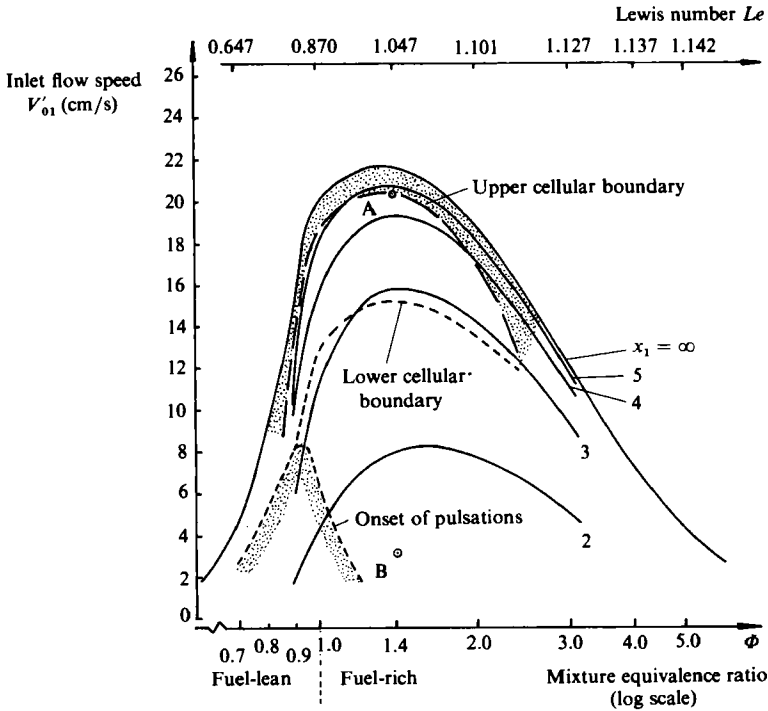


FIGURE 7. Typical plot of inlet flow speed against equivalence for various stand-off distances  $x_{1f}$ . See text (§5) for basic data used. Curves roughly correspond to propane/air mixture burning on porous-plug burner. Shaded regions correspond to cellular boundary (near-adiabatic conditions) and onset of pulsations (at low speeds). Upper cellular boundary is shown to be accurate within limitations of approximate, small-wavenumber theory, but lower cellular boundary is shown to be inaccurate by same limitations. Points A and B at  $\phi = 1.4$  correspond to where  $k_{crit}$  for cellularity = 0.2 (see discussion in text).

numbers in the range  $Le = 0.5-1.5$ . However, the Darcy constants  $\Omega_1, \Omega_2$  are increasing and have a destabilizing influence, and eventually instabilities become apparent just before adiabatic conditions are reached. To demonstrate this, we have considered typical plots of inlet speed against equivalence ratio for a steady flat flame near a flameholder, where the adiabatic stoichiometric speed is taken as  $U'_{o1} = 20$  cm/s, and the dilution factor is taken to be 7. The stoichiometric adiabatic temperature is 1500 K, the gas expansion parameter  $B_1^*$  at adiabatic conditions is 0.8, and the dimensional activation energy is taken to be 40000 cal/mol. Using the formula derived in the work of Clarke & McIntosh (1980), the inlet speed is plotted against equivalence ratio for  $x_{1f} = 2, 3, 4, 5$  and  $\infty$  (adiabatic conditions). The Lewis number is considered to vary with equivalence ratio from 0.58 (fuel lean) to 1.16 (fuel rich) and thus roughly represents a propane/air mixture (see I and Pelcé & Clavin 1982). To estimate the Lewis number at mixtures between these extremes, the formula suggested by Joulin & Mitani (1981) for order-2 reactions is adopted. By setting a value for the thermal diffusivity, Prandtl number, and the pore radius at the holder, one can then use the theory of this paper to establish the critical wavenumber (if any) for cellular instabilities to occur. The onset of such conditions is indicated in figure 7, for  $Pr = 0.75$ ,  $K'_{o1} = 0.3$  cm s<sup>-2</sup> and  $d' = 0.01$  cm, by the shaded area just below adiabatic conditions. The Darcy constants in the transverse and longitudinal directions are assumed equal and the porosity is set at 0.75. At the

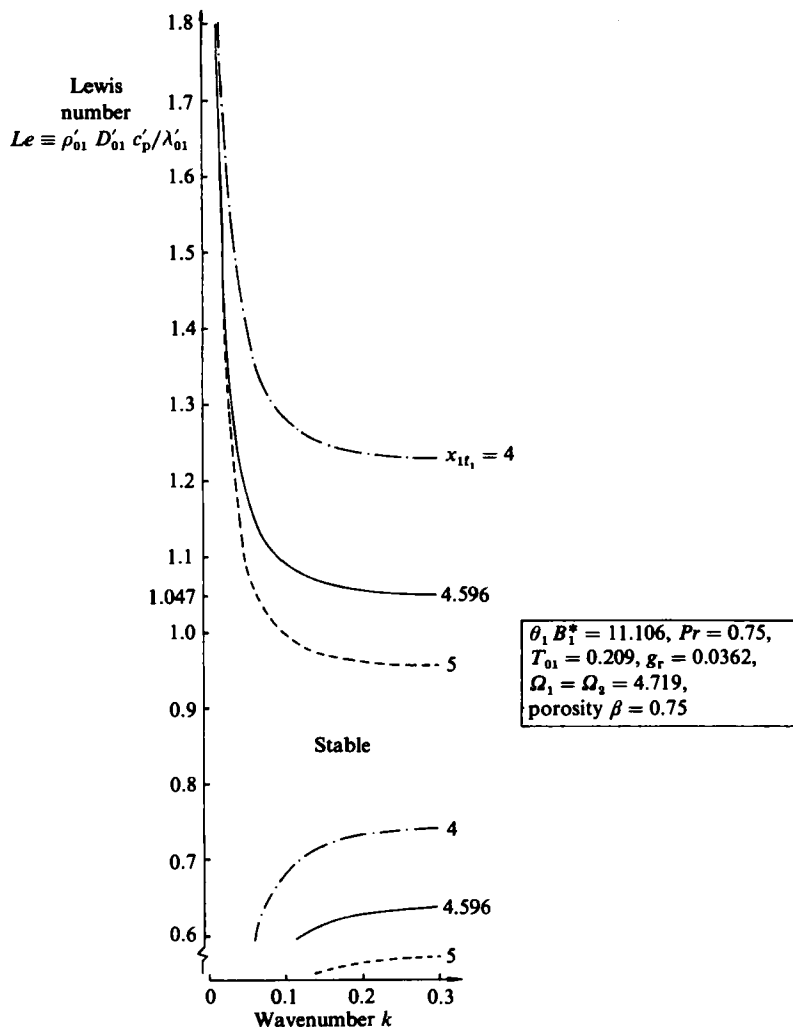


FIGURE 8. Variation of neutral-stability curves with  $x_{1f_1}$  near upper cellular boundary of figure 7;  $\Phi = 1.4$  ( $Le = 1.047$ ).

onset of instability, owing to the approximate nature of the theory, only the initial part of the U-shaped (exact) curve is obtained (see figure 2), so that the wavenumber for the onset of cellularity (i.e. the value at the minimum) cannot be accurately obtained. If the preheat equations were solved exactly, then a definite value could be found corresponding to minima like those illustrated in figure 2. Nevertheless, even for this approximate theory, the critical Lewis number for the onset of cellularity can be determined, and figure 7 clearly demonstrates the region where the cellular instability is to be expected. Figure 8 is a detail of how this occurs in  $(Le, k)$ -space at  $\Phi = 1.4$  ( $Le = 1.047$ ) where the critical  $x_{1f_1}$  value is 4.596. One observes that near this upper stability point,  $x_{1f_1}$  is increasing rapidly with inlet speed and that as  $x_{1f_1}$  increases (e.g. see  $x_{1f_1} = 5$  curve), so the  $k_{crit}$  value quickly comes down to small (and hence more accurate values). One should note that the dimensional stand-off distance can still be small in this region (McIntosh & Clarke 1984a). Figure 8 also serves to demonstrate that there can be a lower neutral stability curve (see the two parts of

the curve for  $x_{1f_1} = 4$  and 4.596). However, as can be seen from the figure as  $x_{1f_1}$  increases, this part of the curve shifts below accessible  $Le$ -values, so that it does not generally affect upper instability predictions.

Figure 7 is important because it confirms the experimental observations of Botha & Spalding (1954), who found cellularity *throughout the stoichiometric range* as adiabatic conditions were approached (see also figure 5 of Clarke & McIntosh (1980), which illustrates the experimental stability boundary in a  $U'_{01}/\tilde{\Phi}$ -plot). Botha & Spalding (1954, p. 94) came to the conclusion that preferential diffusion could not be the sole mechanism governing these flame irregularities and Markstein (1964, p. 77) speculates on the reason for the observations by Botha & Spalding. He attributes the cellular instabilities in their experiments to be due to the influence of the porous flameholder. In that work, he suggests transverse temperature variations across the flameholder surface were responsible. However, since generally the conductance is large, temperature fluctuations will be negligible. Thus the theory put forward in this paper is that *hydrodynamic influences within the holder cause such cellularities to occur*, and the similarity of figure 7 to Botha & Spalding's results substantiates this.

Further investigations into the cause of the upper cellular instability showed clearly the importance of a non-zero value of  $\Omega_2$  (the Darcy constant in the transverse direction i.e. the imposed 'strain' on the flow). The onset of cellularity is much the same as  $\Omega_2/\Omega_1$  is reduced from 1.0 to 0.1. However, once this ratio becomes lower than about 0.1, the neutral-stability line in figure 7 draws noticeably closer to the adiabatic curve. Finally, if  $\Omega_2$  is set to zero, the instability can no longer be found. This finding indicates that cellularity will be more readily observable on porous-plug-type flameholders than with holders of the hypodermic type (where transverse velocities in the holder are not allowed). This is in agreement with observations. Schimmer & Vortmeyer (1977) performed experiments with a flat flame near a burner constructed of small copper tubes. They found that for all subadiabatic speeds flat flames could be stabilized. Only at superadiabatic conditions (beyond the scope of this theory) did the flame become wrinkled. In that subadiabatic cellularity is predicted quite strongly for  $\Omega_2/\Omega_1$  as small as 0.1 (with little change for higher values), it is to be expected, as long as a flameholder is of the porous-plug type, that cellularity will always be observed just before adiabatic conditions are reached.

Figure 7 also has a lower stability boundary which was not observed in Botha & Spalding's experiments. In figure 9, the neutral-stability curves near this point for  $\tilde{\Phi} = 1.4$  ( $Le = 1.407$ ) are shown. One observes that at these low values of  $x_{1f_1}$  the *lower* part of the neutral-stability curve takes prominence, and it is from this part of the curve that instabilities are predicted. However, as  $x_{1f_1}$  goes below the critical value (here  $x_{1f_1} = 2.630$ ) the  $k_{crit}$  values are larger than those in the region beyond the upper stability boundary, so that the results will not be reliable for this essentially small- $k$  approximation. To illustrate this point, we have located two points at  $\tilde{\Phi} = 1.4$  where  $k_{crit} = 0.2$  (and thus comes within acceptable bounds of accuracy). Point A is only very slightly beyond the upper neutral-stability boundary, indicating that this boundary is an accurate prediction of the onset of cellularity. However, point B is well below the lower stability boundary. In the region between the boundary and point B the  $k_{crit}$  values are above 0.2, and thus both the existence and position of the lower neutral stability curve is doubtful from this approximate (small- $k$ ) theory.

We also show some predictions of the planar theory using equation (148) of I (equivalent to (75) of this paper with  $k = 0$ ). For the parameter values used in figure 7, the onset of pulsating instabilities is predicted to occur at low speeds under fuel-lean conditions (see left-hand shaded region on figure 7). The boundary will tend to shift

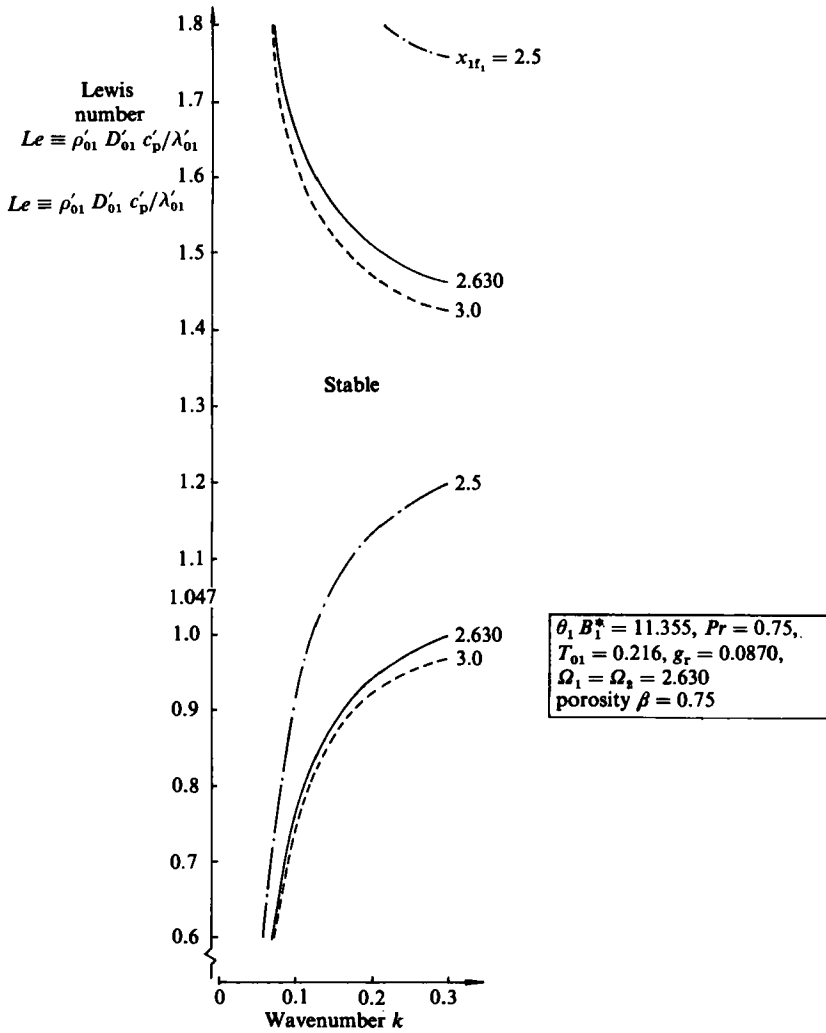


FIGURE 9. Variation of neutral-stability curves with  $x_{1f_1}$  near lower cellular boundary of figure 7;  $\Phi = 1.4$  ( $Le = 1.047$ ).

upwards and further towards fuel-rich conditions when the activation energy is larger. In the region of this boundary travelling waves will be expected to occur (where  $\omega = i\hat{\omega}, k \neq 0$ ), which is in general agreement with Botha & Spalding (1954, p. 93), who indicated that at low speeds waves or rings were formed. The numerical work of Margolis (1980) also substantiates this prediction.

*Free-flame limit*

At each mixture strength we have shown that cellular instabilities are predicted just before adiabatic conditions are reached. It is important to realize that large values of  $x_{1f_1}$  do not necessarily mean that the actual stand off distance of the flame is more than a few millimetres (see McIntosh & Clarke 1984a). Thus the flameholder hydrodynamics have a considerable effect for inlet speeds quite close to adiabatic conditions.

In general, (122) is a complicated function of  $g_r, T_{01}, Le, Pr, \Omega_1, \Omega_2$  as  $x_{1f_1}$  gets large.

There is, however, a useful comparison with the work of previous authors when  $g_r = \Omega_1 = \Omega_2 = 0$ . In the limit  $x_{1f_1} = \infty$  one then obtains a much-simplified version of (122):

$$\left[ \frac{1}{Le} \left( 1 - \frac{1}{Le} \right) + \frac{2}{Le^2 (\theta_1 B_1^*)} \right] \omega^2 + \frac{2\omega}{Le (\theta_1 B_1^*)} - \left[ Le - 1 - \frac{2}{T_{01} (\theta_1 B_1^*)} \right] \frac{k^2}{Le^2} = 0. \quad (129)$$

The last term in (129) implies a critical Lewis number of

$$Le_{\text{crit}} = 1 + \frac{2}{T_{01} (\theta_1 B_1^*)} \quad (130)$$

for the onset of the cellular instability. This confirms the findings of previous authors (Sivashinsky 1977) using diffusional-thermal theory alone. With  $T_{01} = 1$  (no gas expansion) there is immediate correspondence to the

$$l_{\text{crit}} \equiv \theta_1 B_1^* (Le_{\text{crit}} - 1) = 2, \quad (131)$$

value derived in such theories, the significance of which has been much investigated (Buckmaster & Ludford 1982).

However, this limit is only of passing interest here, since, in reality, the hydrodynamic fluctuations within the porous material of the holder have a strong influence even near adiabatic conditions. For *very* large stand-off distances a large hydrodynamic zone would need to be added downstream of the holder and ahead of the preheat zone (similar to that used in the model of Pelcé & Clavin 1982). Thus we conclude that the fluid dynamics of the flow, whether in the flameholder (burner flames) or in a thick upstream zone (free flames), has a strong influence on flame behaviour.

## 6. Conclusions

The stability of burner flames to two-dimensional disturbances has been investigated with no limitation on gas expansion. Within the porous-plug-type burner, it has been assumed that the mixture obeys Darcy's Law linking velocity and pressure gradient. The problem has been first linearized for small unsteady perturbations. Activation-energy asymptotics have then been applied to reduce the problem to a set of ordinary differential equations with non-constant coefficients and jump conditions across the flame. Small-wavenumber analysis has finally been used to make the preheat equations tractable. A dispersion relation has then been derived and used to predict, in particular, the onset of cellular instability as a function of Lewis number, Prandtl number, activation energy, stand-off distance, gas expansion ratio, gravity and flameholder hydrodynamic characteristics.

A major result in this paper is that the hydrodynamic interference of the porous-plug flameholder has a strong influence on the occurrence of flame cellularity. In particular, the theory predicts the onset of cellularity near adiabatic conditions and throughout the stoichiometric range. This is in accord with the experimental observations of Botha & Spalding (1954). For hypodermic-type holders, where transverse velocities are not allowed, the instability is removed for subadiabatic conditions.

This fact underlines the finding of Pelcé & Clavin (1982) – that diffusional-thermal theory alone cannot explain all experimental observations. In particular, hydrodynamic instabilities play an important part in flame behaviour, and here we have shown that the hydrodynamic zone within porous flameholders often used in experiments, can have a profound influence on the experimental results.



The author is grateful to the Science and Engineering Research Council for financial support during the course of this investigation.

The author is also greatly indebted to Professor J. F. Clarke for many fruitful discussions and encouragement. The idea of modelling the flow in the holder according to Darcy's Law originated with him.

### Appendix A. The flow within the porous-plug flameholder

Within a porous material the flow can be assumed to obey Darcy's law, which links the pressure gradient with flow velocity (Carman 1956). Thus in the longitudinal direction

$$U'_h = -\Omega'_1 \frac{\partial p'}{\partial x'}, \quad (\text{A } 1)$$

and in the transverse direction

$$V'_h = -\Omega'_2 \frac{\partial p'}{\partial y'}. \quad (\text{A } 2)$$

Continuity implies

$$\frac{\partial \rho'}{\partial t'} + \frac{\partial}{\partial x'} (\rho' U'_h) + \frac{\partial}{\partial y'} (\rho' V'_h) = 0, \quad (\text{A } 3)$$

but assuming that the holder has a large conductance such that temperature (and hence density) fluctuations at the holder surface are absorbed immediately, we are left with the following three equations in non-dimensional form:

$$U_h = -\frac{\Omega_1}{\gamma} \frac{\partial p_{fh}}{\partial x_1}, \quad (\text{A } 4)$$

$$V_h = -\frac{\Omega_2}{\gamma} \frac{\partial p_{fh}}{\partial y}, \quad (\text{A } 5)$$

$$\frac{\partial U_h}{\partial x_1} + \frac{\partial V_h}{\partial y} = 0. \quad (\text{A } 6)$$

Note that the non-dimensionalization follows that given in §2 of the main text and that

$$\Omega_1 \equiv \Omega'_1 \frac{\rho'_{01} u'^2_{01}}{D'_{01}}, \quad \Omega_2 \equiv \Omega'_2 \frac{\rho'_{01} u'^2_{01}}{D'_{01}}. \quad (\text{A } 7a, b)$$

The subscript 'h' in (A 3)–(A 5) refers to quantities within the holder. At the downstream surface the transverse velocity and pressure are assumed to be continuous, but the longitudinal velocity is reduced by a porosity factor  $\beta$ , which is less than unity. Thus

$$U_h(x_1 = 0) = \beta, \quad (\text{A } 8)$$

$$V_h(x_1 = 0) = V(x_1 = 0), \quad (\text{A } 9)$$

$$p_{fh}(x_1 = 0) = p_f(x_1 = 0). \quad (\text{A } 10)$$

If we now consider perturbations of the form

$$U_h = U_{h(\text{steady})} + \epsilon U_{uh} \exp(iky + \omega t), \quad (\text{A } 11)$$

$$V_h = \epsilon V_{uh} \exp(iky + \omega t), \quad (\text{A } 12)$$

$$p_{fh} = p_{fh(\text{steady})} + \epsilon p_{uh} \exp(iky + \omega t), \quad (\text{A } 13)$$

then we obtain the equation set

$$U_{\text{uh}} = -\frac{\Omega_1}{\gamma} \frac{dp_{\text{uh}}}{dx_1}, \quad (\text{A } 14)$$

$$V_{\text{uh}} = -ik \frac{\Omega_2}{\gamma} p_{\text{uh}}, \quad (\text{A } 15)$$

$$\frac{dU_{\text{uh}}}{dx_1} = -ik V_{\text{uh}}. \quad (\text{A } 16)$$

On the assumption that the length of the porous region is large (compared with diffusion lengths), the solution to these equations is given by

$$U_{\text{uh}} = -k(\Omega_1 \Omega_2)^{\frac{1}{2}} \frac{p_{\text{u}}(0)}{\gamma} \exp \left[ k \left( \frac{\Omega_2}{\Omega_1} \right)^{\frac{1}{2}} x_1 \right], \quad (\text{A } 17)$$

$$V_{\text{uh}} = -ik \Omega_2 \frac{p_{\text{u}}(0)}{\gamma} \exp \left[ k \left( \frac{\Omega_2}{\Omega_1} \right)^{\frac{1}{2}} x_1 \right], \quad (\text{A } 18)$$

$$\frac{p_{\text{uh}}}{\gamma} = \frac{p_{\text{u}}(0)}{\gamma} \exp \left[ k \left( \frac{\Omega_2}{\Omega_1} \right)^{\frac{1}{2}} x_1 \right]. \quad (\text{A } 19)$$

Using the conditions (A 8)–(A 10) at the downstream interface, we then have the results

$$U_{\text{u}}(0) = -\Omega_3 k \frac{p_{\text{u}}(0)}{\gamma}, \quad (\text{A } 20)$$

$$V_{\text{u}}(0) = -\Omega_2 k \frac{p_{\text{u}}(0)}{\gamma}, \quad (\text{A } 21)$$

where

$$\Omega_3 \equiv \beta(\Omega_1 \Omega_2)^{\frac{1}{2}}. \quad (\text{A } 22)$$

These are the results (15*a*), (16) and (17) in the main text.

It remains to estimate a value for  $\Omega'_1$ . Using a simple approach to the flow in the porous material, Clarke (1984) derived the following relationship between  $\Omega'_1$  and the dynamic viscosity coefficient  $\mu'_{01}$ :

$$\Omega'_1 = \frac{8d'^2}{\mu'_{01}}, \quad (\text{A } 23)$$

where  $d'$  is a measure of the pore diameter. More-general formulae can be derived (see Carman 1956), but they only alter the proportionality factor. The essential feature is the proportionality to  $d'^2$  and the inverse of  $\mu'_{01}$ . We adopt this simple relationship here, and observe from (A 7*a*) that

$$\Omega_1 = \frac{8d'^2}{\mu'_{01}} \frac{\rho'_{01} u'^2_{01}}{D'_{01}} = \frac{8d'^2 u'^2_{01}}{Le Pr K'^2_{01}}, \quad (\text{A } 24)$$

where  $K'_{01}$  is the thermal diffusivity and  $Le$  and  $Pr$  are Lewis and Prandtl numbers. Equation (A 24) corresponds to (18) in the main text.

In practice,  $d'$ ,  $\beta$  and the ratio  $\Omega_2/\Omega_1$  will be specified at the holder. For the results illustrated in this paper  $\beta$  was set at 0.75 and the ratio  $\Omega_2/\Omega_1$  set to unity.  $d'$  was usually taken to be 0.01 cm.

## Appendix B. Jump conditions across the flame

The derivation of the jump conditions across the flame follows closely that given in detail in I with an extension to two dimensions. Therefore we only summarize the method here. Inner series expansions are sought for  $T_u$ ,  $C_{\ell u}$ ,  $U_u$ ,  $H_u$  and  $W_u$  in ascending powers of  $\theta_1^{-1}$ .

$$T_u = -\mathcal{T}_u^{(0)}(X) - \frac{1}{\theta_1} \mathcal{T}_u^{(1)}(X) - \frac{1}{\theta_1^2} \mathcal{T}_u^{(2)}(X) - \dots, \quad (\text{B } 1)$$

$$C_{\ell u} = \overline{\mathcal{C}}_u^{(0)}(X) + \frac{1}{\theta_1} \overline{\mathcal{C}}_u^{(1)}(X) + \frac{1}{\theta_1^2} \overline{\mathcal{C}}_u^{(2)}(X) + \dots, \quad (\text{B } 2)$$

$$U_u = \mathcal{U}_u^{(0)}(X) + \frac{1}{\theta_1} \mathcal{U}_u^{(1)}(X) + \frac{1}{\theta_1^2} \mathcal{U}_u^{(2)}(X) + \dots, \quad (\text{B } 3)$$

$$V_u = \mathcal{V}_u^{(0)}(X) + \frac{1}{\theta_1} \mathcal{V}_u^{(1)}(X) + \frac{1}{\theta_1^2} \mathcal{V}_u^{(2)}(X) + \dots, \quad (\text{B } 4)$$

$$H_u = \mathcal{H}_u^{(0)}(X) + \frac{1}{\theta_1} \mathcal{H}_u^{(1)}(X) + \frac{1}{\theta_1^2} \mathcal{H}_u^{(2)}(X) + \dots, \quad (\text{B } 5)$$

$$W_u = \mathcal{W}_u^{(0)}(X) + \frac{1}{\theta_1} \mathcal{W}_u^{(1)}(X) + \frac{1}{\theta_1^2} \mathcal{W}_u^{(2)}(X) + \dots, \quad (\text{B } 6)$$

where the inner variable  $X$  is defined by

$$X \equiv \theta_1(x_1 - x_{1f}), \quad (\text{B } 7)$$

and the expansions of the steady variables  $T_s$ ,  $C_{\ell s}$  are given by

$$T_s = 1 - \frac{1}{\theta_1} \mathcal{T}_s^{(1)}(X) - \dots, \quad \overline{C}_{\ell s} = \frac{1}{\theta_1} \overline{\mathcal{C}}_s^{(1)}(X) + \dots \quad (\text{B } 8a, b)$$

Substitution of these series expansions into (33)–(37) of the main text reveals (via the longitudinal momentum equation) the gauge functions necessary for the pressure expansion. It is found that to balance the other terms,  $p_u$  must be of the form

$$p_u = \theta_1 \mathcal{P}_u^{(0)}(X) + \mathcal{P}_u^{(1)} + \dots \quad (\text{B } 9)$$

This expansion appears superficially to be inconsistent with the other parts of the analysis, but is in fact entirely correct. It should be remembered that the inner-zone behaviour is different for  $\epsilon \ll \theta_1^{-1}$  (here) than when one assumes  $\epsilon \gg \theta_1^{-1}$ . It is helpful here to reconstruct the full pressure variable; from (1) and (30) of the main text, we have, in the inner zone,

$$P = 1 + M^2 \left\{ \left( \mathcal{P}^{(1)} + O\left(\frac{1}{\theta_1}\right) \right) + \epsilon \exp(\omega t + iky) \left[ \theta_1 \mathcal{P}_u^{(0)} + \mathcal{P}_u^{(1)} + O\left(\frac{1}{\theta_1}\right) \right] \right\}, \quad (\text{B } 10)$$

where  $\mathcal{P}^{(1)}$  comes from the expansion of the steady pressure,

$$p_s = \mathcal{P}^{(1)}(X) + \frac{1}{\theta_1} \mathcal{P}^{(2)}(X) + \dots \quad (\text{B } 11)$$

The steady theory in fact shows that

$$\frac{\mathcal{P}^{(1)}}{\gamma} = -\frac{4Sc}{3T_{01}} \frac{d\mathcal{T}^{(1)}}{dX} + \text{const.}, \quad (\text{B } 12)$$

where (see I) we know that

$$\frac{d\mathcal{F}^{(1)}}{dX} = -Le B_1 g, \quad g(\mathcal{F}^{(1)}) \equiv [1 - e^{-\mathcal{F}^{(1)}}(1 + \mathcal{F}^{(1)})]^{\frac{1}{2}}. \quad (\text{B } 13a, b)$$

Equation (B 10) shows that the leading term of the perturbation is  $O(\theta_1 \epsilon)$ , but since we have specifically taken the distinguished limit

$$\theta_1 \epsilon \rightarrow 0 \quad \text{as } \epsilon \rightarrow 0, \quad (\text{B } 14)$$

the  $\theta_1 \epsilon$  term is acceptable. This underlines the different character of the inner reaction zone under the two limits  $\theta_1 \epsilon \rightarrow 0$  and  $\theta_1 \epsilon \rightarrow \infty$ .

It is then found upon substitution that the leading-order terms satisfy the following differential equations;

$$\frac{d^2 \mathcal{F}_u^{(0)}}{dX^2} = \frac{1}{2} Le B_1^2 (\bar{\mathcal{C}}_u^{(0)} - \bar{\mathcal{C}}^{(1)} \mathcal{F}_u^{(0)}) e^{-\mathcal{F}^{(1)}}, \quad (\text{B } 15)$$

$$\frac{d^2 \mathcal{C}_u^{(0)}}{dX^2} = \frac{1}{2} Le^2 B_1^2 (\bar{\mathcal{C}}_u^{(0)} - \bar{\mathcal{C}}^{(1)} \mathcal{F}_u^{(0)}) e^{-\mathcal{F}^{(1)}}, \quad (\text{B } 16)$$

$$\frac{d\mathcal{U}_u^{(0)}}{dX} = -\frac{1}{T_{01}} \frac{d\mathcal{F}_u^{(0)}}{dX}, \quad (\text{B } 17)$$

$$\frac{d^2 \mathcal{V}_u^{(0)}}{dX^2} = 0, \quad (\text{B } 18)$$

$$\frac{1}{\gamma} \frac{d\mathcal{P}_u^{(0)}}{dX} = \frac{4}{3} Sc \frac{d^2 \mathcal{U}_u^{(0)}}{dX^2}. \quad (\text{B } 19)$$

The preheat and equilibrium variables are also given series expansions in the form

$$\Theta_u = \Theta_{up}^{(1)} + \frac{\Theta_{up}^{(2)}}{\theta_1} + \dots \quad [\Theta = T, C_t, U, V, p, H, W], \quad (\text{B } 20)$$

$$\Phi_u = \Phi_{ue}^{(0)} + \frac{\Phi_{ue}^{(1)}}{\theta_1} + \dots \quad [\Phi = T, U, V, p, H, W], \quad (\text{B } 21)$$

(where superscripts maintain consistency with notation in I and previous papers) and it is found that

$$\mathcal{W}_u^{(0)} = W_{up}^{*(1)} = ik \int_0^{x_{1f_1}} V_{up}^{(1)} dx_1 \quad (= \text{const.}), \quad (\text{B } 22)$$

$$\mathcal{X}_u^{(0)} = H_{up}^{*(1)} = -ik \int_0^{x_{1f_1}} T_{up}^{(1)} dx_1 \quad (= \text{const.}), \quad (\text{B } 23)$$

where \* denotes evaluation at  $x_1 = x_{1f_1}$ .

Integration of (B 15)–(B 19) yields

$$\mathcal{F}_u^{(0)} = -T_{up}^{*(1)} g(\mathcal{F}^{(1)}), \quad (\text{B } 24)$$

$$\bar{\mathcal{C}}_u^{(0)} = \frac{\mathcal{F}_u^{(0)}}{Le}, \quad (\text{B } 25)$$

$$\mathcal{U}_u^{(0)} = U_{ue}^{*(0)} - \frac{\mathcal{F}_u^{(0)}}{T_{01}}, \quad (\text{B } 26)$$

$$\mathcal{V}_u^{(0)} = V_{up}^{*(1)} = V_{ue}^{*(0)} = \text{const.}, \quad (\text{B } 27)$$

$$\frac{\mathcal{P}_u^{(0)}}{\gamma} = \frac{4Sc}{3} \frac{d\mathcal{U}_u^{(0)}}{dX} = -\frac{2Pr B_1}{3T_{01}} T_{up}^{*(1)} \mathcal{F}^{(1)} e^{-\mathcal{F}^{(1)}}. \quad (\text{B } 28)$$

We observe that just as under steady conditions  $\mathcal{P}^{(1)}$  followed  $d\mathcal{T}^{(1)}/dX$ , so also, under unsteady conditions,  $\mathcal{P}_u^{(0)}$  follows  $d\mathcal{T}_u^{(0)}/dX$ . Notice that  $\mathcal{P}_u^{(0)}$  is zero on *both* sides of the flame (equilibrium  $\mathcal{T}^{(1)} = 0$ ; preheat  $\mathcal{T}^{(1)} = \infty$ ), but that in the flame itself there is a non-zero contribution from  $\mathcal{P}_u^{(0)}$ .

Matching of (B 25) and (B 26) to the preheat and equilibrium solutions gives

$$\overline{C}_{up}^{*(1)} + \frac{1}{Le} T_{up}^{*(1)} = 0, \quad (\text{B } 29)$$

$$U_{up}^{*(1)} - U_{ue}^{*(0)} = \frac{1}{T_{01}} T_{up}^{*(1)}. \quad (\text{B } 30)$$

The next-order terms in the inner zone satisfy the following set of differential equations:

$$-\omega \mathcal{T}_u^{(0)} - \frac{d\mathcal{T}_u^{(1)}}{dX} + W_{up}^{*(1)} \frac{d\mathcal{T}^{(1)}}{dX} - T_{01} \frac{d\mathcal{Y}_u^{(1)}}{dX} - ik\mathcal{V}_u^{(0)} = 0, \quad (\text{B } 31)$$

$$-\frac{d\mathcal{T}_u^{(0)}}{dX} + \frac{1}{Le} \frac{d^2\mathcal{T}_u^{(1)}}{dX^2} = \mathcal{R}, \quad (\text{B } 32)$$

$$\frac{d\overline{\mathcal{C}}_u^{(0)}}{dX} - \frac{d^2\overline{\mathcal{C}}_u^{(1)}}{dX^2} = -\mathcal{R}, \quad (\text{B } 33)$$

$$\frac{d\mathcal{Y}_u^{(0)}}{dX} + \frac{1}{\gamma} \frac{d\mathcal{P}_u^{(0)}}{dX} = \frac{4}{3} Sc \frac{d^2\mathcal{Y}_u^{(1)}}{dX^2}, \quad (\text{B } 34)$$

$$\frac{ik\mathcal{P}_u^{(0)}}{\gamma T_{01}} - \frac{Sc H_{up}^{*(1)}}{T_{01}^2} \frac{d^2\mathcal{T}^{(1)}}{dX^2} = Sc \frac{d^2\mathcal{V}_u^{(1)}}{dX^2} + \frac{1}{3} \frac{ikSc}{T_{01}} \frac{d\mathcal{Y}_u^{(0)}}{dX}, \quad (\text{B } 35)$$

where the  $\mathcal{R}$ -term (see I; equations (91) and (92)) is given by

$$\begin{aligned} \mathcal{R} = & \frac{1}{2} Le^2 B_1^2 e^{-\mathcal{T}^{(1)}} \left[ A_1^{(2)} (\overline{\mathcal{C}}_u^{(0)} - \overline{\mathcal{C}}^{(1)} \mathcal{T}_u^{(0)}) - (\mathcal{T}^{(2)} + \mathcal{T}^{(1)^2} (\overline{\mathcal{C}}_u^{(0)} - \overline{\mathcal{C}}^{(1)} \mathcal{T}_u^{(1)})) \right. \\ & \left. + \frac{2\sigma \overline{\mathcal{C}}^{(1)} \mathcal{T}_u^{(0)}}{Le(1+\sigma)Q_1|A_1|} - \overline{\mathcal{C}}^{(1)} \mathcal{T}_u^{(1)} + \overline{\mathcal{C}}_u^{(1)} - \frac{\sigma \mathcal{T}_u^{(0)} \overline{\mathcal{C}}^{(1)^2}}{(1+\sigma)Q_1|A_1|} - \mathcal{T}_u^{(0)} \overline{\mathcal{C}}^{(2)} - 2\mathcal{T}_u^{(0)} \mathcal{T}^{(1)} \overline{\mathcal{C}}^{(1)} \right], \end{aligned} \quad (\text{B } 36)$$

and it should be noted that  $A_1$  (the pre-exponential eigenvalue) is expanded as

$$A_1 = \theta_1^2 A_1^{(1)} \left( 1 + \frac{A_1^{(2)}}{\theta_1} + \dots \right), \quad (\text{B } 37)$$

with

$$A_1^{(1)} = \frac{Le B_1^2}{2|A_1|}, \quad (\text{B } 38)$$

$$A_1^{(2)} = 2 \left[ 3 - \frac{J}{B_1} - \frac{\sigma}{Le(1+\sigma)Q_1|A_1|} - \frac{1}{B_1} \left( 1 - \frac{1}{Le} \right) \right], \quad (\text{B } 39)$$

$$J \equiv \int_0^\infty [1 - g(m)] dm = 1.344\dots \quad (\text{B } 40)$$

The equation at the next order ( $O(1)$ ) obtained by eliminating the reaction term is also required. Using relationships satisfied by the steady solution, this can be simplified to

$$-\omega \mathcal{T}_u^{(0)} \left( 1 - \frac{1}{Le} \right) - \frac{d\mathcal{T}_u^{(1)}}{dX} + \frac{d\overline{\mathcal{C}}_u^{(1)}}{dX} + \frac{1}{Le} \frac{d^2\mathcal{T}_u^{(2)}}{dX^2} - \frac{d^2\overline{\mathcal{C}}_u^{(2)}}{dX^2} + W_{up}^{*(1)} \left( 1 - \frac{1}{Le} \right) \frac{d\mathcal{T}^{(1)}}{dX} = 0. \quad (\text{B } 41)$$

Dealing first with the temperature and species equations, elimination of the reaction term between (B 32) and (B 33) and integrating once across the reaction zone yields

$$\overline{C_{\text{up}}^{*(1)}} + T_{\text{up}}^{*(1)} = \frac{d\overline{C_{\text{up}}^{(1)}}}{dx_1} \Big|_{r_1} + \frac{1}{Le} \frac{dT_{\text{up}}^{(1)}}{dx_1} \Big|_{r_1}. \quad (\text{B } 42)$$

Two integrations of the same equation, again using matching on both sides of the flame, yields

$$\overline{C_{\text{up}}^{*(2)}} + \frac{1}{Le} T_{\text{up}}^{*(2)} = \frac{1}{Le} T_{\text{ue}}^{*(1)}. \quad (\text{B } 43)$$

The direct integration of (B 32) is detailed in I, where it is shown that the following condition holds:

$$\frac{1}{Le B_1} \frac{dT_{\text{up}}^{(1)}}{dx_1} \Big|_{r_1} = \frac{1}{B_1} T_{\text{up}}^{*(1)} + \frac{1}{2} T_{\text{ue}}^{*(1)}. \quad (\text{B } 44)$$

Lastly, one integration of (B 41) across the reaction zone gives

$$(\overline{C_{\text{up}}^{*(2)}} + T_{\text{up}}^{*(2)}) - \left( \frac{d\overline{C_{\text{up}}^{(2)}}}{dx_1} \Big|_{r_1} + \frac{1}{Le} \frac{dT_{\text{up}}^{(2)}}{dx_1} \Big|_{r_1} \right) = \left( T_{\text{ue}}^{*(1)} - \frac{1}{Le} \frac{dT_{\text{ue}}^{(1)}}{dx_1} \Big|_{r_1} \right). \quad (\text{B } 45)$$

We thus observe that by reconstructing the full expressions on both sides of the flame, (B 29) and (B 43) are consistent with the jump condition

$$\overline{C_{\text{up}}^*} + \frac{1}{Le} T_{\text{up}}^* = \frac{1}{Le} T_{\text{ue}}^*, \quad (\text{B } 46)$$

and (B 44) is consistent with the jump condition

$$\frac{1}{Le B_1} \frac{dT_{\text{up}}}{dx_1} \Big|_{r_1} = \frac{1}{B_1} T_{\text{up}}^* + \frac{1}{2} \theta_1 T_{\text{ue}}^*. \quad (\text{B } 47)$$

Results (B 42) and (B 45) combine to give the jump condition

$$(\overline{C_{\text{up}}^*} + T_{\text{up}}^*) - \left( \frac{d\overline{C_{\text{up}}}}{dx_1} \Big|_{r_1} + \frac{1}{Le} \frac{dT_{\text{up}}}{dx_1} \Big|_{r_1} \right) = \left( T_{\text{ue}}^* - \frac{1}{Le} \frac{dT_{\text{ue}}}{dx_1} \Big|_{r_1} \right). \quad (\text{B } 48)$$

Thus conditions (46)–(48) of the main text have thus been justified up to  $O(\theta_1^{-1})$  terms. Note that  $T_{\text{ue}}^{(0)} = 0$  (see I).

We now go on to consider the continuity (B 31) and momentum equations (B 34 and B 35). Integration of the longitudinal momentum equation (B 34) across the reaction zone yields

$$(U_{\text{up}}^{*(1)} - U_{\text{ue}}^{*(0)}) + \frac{1}{\gamma} (p_{\text{up}}^{*(1)} - p_{\text{ue}}^{*(0)}) = \frac{4}{3} Sc \left( \frac{dU_{\text{up}}^{(1)}}{dx_1} \Big|_{r_1} - \frac{dU_{\text{ue}}^{(0)}}{dx_1} \Big|_{r_1} \right), \quad (\text{B } 49)$$

and in a similar manner integration of the transverse momentum equation (B 35) gives

$$\frac{dV_{\text{up}}^{(1)}}{dx_1} \Big|_{r_1} - \frac{dV_{\text{ue}}^{(0)}}{dx_1} \Big|_{r_1} = \frac{1}{T_{01}^2} (Le B_1 H_{\text{up}}^{*(1)} + ik T_{\text{up}}^{*(1)}). \quad (\text{B } 50)$$

Integration of the continuity equation (B 31) yields

$$(U_{\text{up}}^{*(2)} - U_{\text{ue}}^{*(1)}) = \frac{1}{T_{01}} (T_{\text{up}}^{*(2)} - T_{\text{ue}}^{*(1)}). \quad (\text{B } 51)$$

Two integrations of the transverse momentum equation (B 35) yield (upon matching)

$$V_{\text{up}}^{*(2)} = V_{\text{ue}}^{*(1)}, \quad (\text{B } 52)$$

and we lastly consider the inner-zone momentum equations at  $O(1)$  level. These are given by

$$\begin{aligned} \omega \mathcal{Q}_u^{(0)} + \frac{d\mathcal{Q}_u^{(1)}}{dX} + \frac{1}{\gamma} \frac{d\mathcal{P}_u^{(2)}}{dX} + \frac{W_{up}^{*(1)}}{T_{01}} \frac{d\mathcal{F}^{(0)}}{dX} \\ = \frac{4}{3} Sc \frac{d\mathcal{Q}_u^{(2)}}{dX^2} + \frac{2}{3} \frac{Sc ik}{T_{01}} V_{up}^{*(1)} \frac{d\mathcal{F}^{(1)}}{dX} \\ - \frac{1}{3} \frac{Sc ik}{T_{01}} \frac{d\mathcal{V}_u^{(1)}}{dX} - \frac{Sc}{T_{01}^2} \left( \frac{ik}{T_{01}} H_{up}^{*(1)} \frac{d\mathcal{F}^{(1)}}{dX} + k^2 \mathcal{Q}_u^{(0)} \right), \end{aligned} \quad (B 53)$$

$$\begin{aligned} \omega V_{up}^{*(1)} + \frac{d\mathcal{V}_u^{(1)}}{dX} + \frac{ik}{\gamma T_{01}} (\mathcal{P}_u^{(1)} - \mathcal{F}^{(1)} \mathcal{P}_u^{(0)}) \\ + \frac{Sc}{T_{01}^2} \left( -H_{up}^{*(1)} \frac{d^2 \mathcal{F}^{(2)}}{dX^2} - \mathcal{H}_u^{(1)} \frac{d^2 \mathcal{F}^{(1)}}{dX^2} + H_{up}^{*(1)} \mathcal{F}^{(1)} \frac{d^2 \mathcal{F}^{(1)}}{dX^2} \right) \\ - \frac{H_{up}^{*(1)}}{T_{01}} g_r + \frac{H_{up}^{*(1)}}{T_{01}^2} \frac{d\mathcal{F}^{(1)}}{dX} \\ = Sc \frac{d^2 \mathcal{V}_u^{(2)}}{dX^2} - \frac{4}{3} \frac{k^2 Sc}{T_{01}^2} V_{up}^{*(1)} - \frac{ik Sc}{T_{01}} \frac{d\mathcal{F}^{(1)}}{dX} \mathcal{Q}_u^{(0)} \\ + \frac{Sc}{T_{01}^2} \frac{d\mathcal{F}^{(1)}}{dX} \left[ \frac{d\mathcal{H}_u^{(1)}}{dX} + H_{up}^{*(1)} \frac{d\mathcal{F}^{(1)}}{dX} \right] \\ + \frac{1}{3} \frac{ik Sc}{T_{01}} \left[ \frac{d\mathcal{Q}_u^{(1)}}{dX} - \mathcal{F}^{(1)} \frac{d\mathcal{Q}_u^{(0)}}{dX} \right]. \end{aligned} \quad (B 54)$$

Integration of (B 53) yields

$$(U_{up}^{*(2)} - U_{ue}^{*(1)}) + \frac{1}{\gamma} (p_{up}^{*(2)} - p_{ue}^{*(1)}) = \frac{4}{3} Sc \left( \frac{dU_{up}^{(2)}}{dx_1} \Big|_{r_1} - \frac{dU_{ue}^{(1)}}{dx_1} \Big|_{r_1} \right), \quad (B 55)$$

and in a similar manner, after much (lengthy) substitution, integration of (B 54) gives

$$\frac{dV_{up}^{(2)}}{dx_1} \Big|_{r_1} - \frac{dV_{ue}^{(1)}}{dx_1} \Big|_{r_1} = \frac{1}{T_{01}^2} [Le B_1 H_{up}^{*(2)} + ik(T_{up}^{*(2)} - T_{ue}^{*(1)})]. \quad (B 56)$$

It should be noted that integration (and matching) of the  $O(\theta_1)$  equations in  $\mathcal{H}_u^{(1)}$ ,  $\mathcal{W}_u^{(1)}$  given by

$$\frac{d\mathcal{H}_u^{(1)}}{dX} + H_{up}^{*(1)} \frac{d\mathcal{F}^{(1)}}{dX} = ik \mathcal{F}_u^{(0)}, \quad (B 57)$$

$$\frac{d\mathcal{W}_u^{(1)}}{dX} = ik V_{up}^{*(1)}, \quad (B 58)$$

yields the simple continuity conditions

$$H_{up}^{*(2)} = H_{ue}^{*(1)}, \quad (B 59)$$

$$W_{up}^{*(2)} = W_{ue}^{*(1)}. \quad (B 60)$$

We now proceed to reconstruct the full expressions on both sides of the flame in exactly the same manner as for (B 46)–(B 48). Results (B 30) and (B 51) are consistent with the jump condition

$$U_{up}^* - U_{ue}^* = \frac{1}{T_{01}} (T_{up}^* - T_{ue}^*), \quad (B 61)$$

and (B 50) and (B 56) combine to give the jump condition

$$\frac{dV_{up}}{dx_1} \Big|_{f_1} - \frac{dV_{ue}}{dx_1} \Big|_{f_1} = \frac{1}{T_{01}^2} [Le B_1 H_u^* + ik(T_{up}^* - T_{ue}^*)]. \quad (\text{B } 62)$$

Results (B 49) and (B 55) yield

$$(U_{up}^* - U_{ue}^*) + \frac{1}{\gamma} (p_{up}^* - p_{ue}^*) = \frac{4}{3} Sc \left( \frac{dU_{up}}{dx_1} \Big|_{f_1} - \frac{dU_{ue}}{dx_1} \Big|_{f_1} \right), \quad (\text{B } 63)$$

and (B 22), (B 23), (B 27), (B 52), (B 59) and (B 60) imply

$$V_{up}^* = V_{ue}^*, \quad H_{up}^* = H_{ue}^*, \quad W_{up}^* = W_{ue}^*. \quad (\text{B } 64a, b, c)$$

Hence, up to  $O(\theta_1^{-1})$  terms, (46)–(51) of the main text have been verified. It is anticipated (though not proven here), that integrating the next-order equations will continue to justify the jump conditions (46)–(51) and that for large  $\theta_1$  these results are a good approximation to the effect of the flame on small-scale perturbations.

#### REFERENCES

- BOTHA, J. P. & SPALDING, D. P. 1954 The laminar flame speed of propane/air mixtures with heat extraction from the flame. *Proc. R. Soc. Lond. A* **225**, 71–96.
- BUCKMASTER, J. D. 1983 Stability of the porous plug burner flame. *SIAM J. Appl. Maths* **43**, 1335–1349.
- BUCKMASTER, J. D. & LUDFORD, G. S. S. 1982 *Theory of Laminar Flames*. Cambridge University Press.
- CARMAN, P. C. 1956 *Flow of Gases Through Porous Media*. Butterworths.
- CLARKE, J. F. 1984 Regular reflections of a weak shock wave from a rigid porous wall. *Q. J. Mech. Appl. Maths* **37**(1), 87–111.
- CLARKE, J. F. & MCINTOSH, A. C. 1980 The influence of a flame-holder on a plane flame including its static stability. *Proc. R. Soc. Lond. A* **372**, 367–392.
- CLAVIN, P. & WILLIAMS, F. A. 1982 Effects of molecular diffusion and of thermal expansion on the structure and dynamics of premixed flames in turbulent flows of large scale and low intensity. *J. Fluid Mech.* **116**, 251–282.
- COFFEE, T. P., KOTLAR, A. J. & MILLER, M. S. 1983 The overall reaction concept in premixed, laminar, steady-state flames. I. Stoichiometries. *Combust. Flame* **54**, 155–169.
- HIRSCHFELDER, J. O., CURTISS, C. F. & BIRD, R. B. 1954 *Molecular Theory of Gases and Liquids*. Wiley.
- JOULIN, G. & MITANI, T. 1981 Linear stability analysis of two-reactant flames. *Combust. Flame* **40**, 235–246.
- KANURY, A. M. 1975 *Introduction to Combustion Phenomena*. Gordon & Breach.
- KASSOY, D. R. 1985 Mathematical modelling for planar, steady, subsonic combustion waves. *Ann. Rev. Fluid Mech.* **17**, 267–287.
- MCINTOSH, A. C. 1984 On the cellular instability of flames near porous-plug burners. Appendix C: Constants for small wavenumber solution. *Cranfield, Coll. of Aero. Rep.* 8427.
- MCINTOSH, A. C. & CLARKE, J. F. 1983 Resonant response of a flat flame near a flame-holder. In *Flames, Lasers and Reactive Systems; AIAA Prog. Series in Astro. Aero.*, vol. 88, pp. 3–37.
- MCINTOSH, A. C. & CLARKE, J. F. 1984a A review of theories currently being used to model steady plane flames on flame-holders. *Combust. Sci. Tech.* **37**, 201–219.
- MCINTOSH, A. C. & CLARKE, J. F. 1984b Second order theory of unsteady burner-anchored flames with arbitrary Lewis number. *Combust. Sci. Tech.* **38**, 161–196.
- MARGOLIS, S. B. 1980 Bifurcation phenomena in burner-stabilized pre-mixed flames. *Combust. Sci. Tech.* **22**, 143–169.



- MARGOLIS, S. B. & KERSTEIN, A. R. 1983 Flame stabilization in a layered medium. *Sandia Natl Labs Rep.* SAND 83-8218.
- MARKSTEIN, G. H. 1964 *Non-Steady Flame Propagation*. Pergamon.
- MATALON, M. & MATKOWSKY, B. J. 1982 Flames as gasdynamic discontinuities. *J. Fluid Mech.* **124**, 239–259.
- PELCÉ, P. & CLAVIN, P. 1982 Influence of hydrodynamics and diffusion upon the stability limits of laminar premixed flames. *J. Fluid Mech.* **124**, 219–237.
- SCHIMMER, H. & VORTMEYER, D. 1977 Acoustical oscillation in a combustion system with a flat flame. *Combust Flame* **28**, 17–24.
- SIVASHINSKY, G. I. 1977 Diffusional–thermal theory of cellular flames. *Combust. Sci. Tech.* **15**, 137–146.